SPENT FUEL SHIPPING CASK

FOR

PM-1 AND PM-3A NUCLEAR POWER PLANTS

HAZARDS SUMMARY EVALUATION

MND-M-1856

THE MARTIN COMPANY

NUCLEAR DIVISION

BALTIMORE, MARYLAND

MAY, 1961

Edited by:

W. P. Haass

Approved by:

G. F. Zindler

DISCLAIMER

LEGAL NOTICE

TABLE OF CONTENTS

CONCLUSIONS

The design of the spent fuel shipping cask proposed for use in transporting irradiated cores from both the PM-1 and PM-3A Nuclear Power Plants has been evaluated under normal and accident conditions. Specifically, the following aspects of the design were analyzed and evaluated:

(1) The lead shielding provided within the walls of the shipping cask and associated attachments assures that ICC regulations of 200 mr/hr at the surface and 10 mr/hr at one meter distance are satisfied.

(2) A rugged crash frame, cask shroud, and shipping pallet combination completely envelopes the cask and insures the structural integrity of the cask under all conditions of transport.

(3) The fuel bundles, control rods, and poison plates are securely locked within the core shroud by means of a core handling fixture with suitable safety devices to guarantee no possible change in core geometry.

(4) Based on an unirradiated core, adequate poisoning in the form of control rods and poison plates is provided to obtain a K_{eff} of less than 0.9 during shipment.

(5) As a result of conservative calculations, sufficient heat transfer capability has been provided in the shipping cask to dissipate 2 kw of heat with coolant temperatures less than 192°F and cask surface temperatures less than 180°F with water coolant present.

(6) Under loss of coolant conditions with only air as a heat transfer medium, it is shown that the peak fuel

temperature is 732°F which is 218°F below the temperature at which sound fuel elements would rupture.

(7) In the event of the remote accident condition in which 5% of the fuel elements are postulated to break into one foot long sections, it is shown that negligible quantities of activity are released to the surrounding environment.

As a result of the foregoing conclusions, the proposed spent fuel shipping cask design is adequate for use in transporting spent cores from both the PM-1 and PM-3A plants to the Idaho Chemical Processing Plant with no undue hazard to the health and safety of operating personnel and the general public.

INTRODUCTION

This Hazards Report presents a description of a lead-shielded spent fuel shipping cask to be employed in transporting spent cores from both the PM-1 and PM-3A Nuclear Power Plants to the Idaho Chemical Processing Plant at Scoville, Idaho. All aspects of the cask design are described in this report including normal and accidental operating conditions. Technical analyses of both the cask design and the core are presented to demonstrate the high degree of safety included in the cask design. The cask design is a result of the efforts of The Edlow Lead Company working in conjunction with Battelle Memorial Institute and with the assistance of the Martin Company.

The design of the spent fuel shipping cask, described herein, is compatible to the requirements of both the PM-1 and PM-3A Nuclear Power Plants. The cores to be transported are identical in every respect. The PM-1 plant is designed to supply the electrical power and space heating requirements for a radar installation at Sundance, Wyoming. The PM-3A plant is designed to provide the electrical power requirements for the Naval Air Facility at McMurdo, Antarctica.

I. DESCRIPTION OF THE SPENT FUEL SHIPPING CASK

The spent fuel shipping cask assembly consists of the following major components: a lead-shielded cask into which the spent core is placed, a steel crash frame surrounding the cask to provide protection in the event of an accidental free fall, a one inch thick steel cylindrical shroud placed around the sides of the cask to provide additional shielding to satisfy ICC Regulations, and an aluminum shipping pallet. These components are described in greater detail below.

A. Spent Fuel Shipping Cask

The spent fuel shipping cask, shown in detail in Martin drawing 372-2106015, consists of lead walls with a maximum thickness of 7 7/8 inches encased in stainless steel. The unnecessary lead shielding at the upper and lower corners is deleted to minimize weight with the result that a contoured wall cross-section is obtained. The lead thickness at the top and bottom of the cask is 8 1/4 inches.

The cavity walls consist of 1/4 inch thick stainless steel. Six stainless steel support blocks are welded to the base of the cavity to provide support for the spent core assembly and allow for the passage of coolant to the core. The cavity walls are contoured to the shape of the spent core assembly to minimize weight.

The outer cask walls consist of 1/2 inch thick stainless steel to which are welded 3 inch deep fins on approximately one inch centers. Approximately 100 such fins are placed vertically around the circumference of the cask to provide the required heat transfer capability. Tie-down points, designed to withstand 8g loads, are

located between pairs of extra heavy and enlarged fins and permit securing the cask both to its shipping pallet and the transport vehicle floor. A pair of trunnions designed to meet the requirements at the Idaho Chemical Processing Plant are provided to facilitate handling.

The cask cover consists of 8 1/4 inches thick lead encased in 1/4 inch thick stainless steel around the sides and bottom and 3/4 inch thick stainless steel on the top. A gasketed seal, designed to withstand an internal pressure of 60 psig, is employed to preclude leakage. The cask, however, will never be operated at pressures greater than atmospheric, although it can withstand 60 psig. The cover is secured to the cask body by means of 12(one inch diameter) bolts and a lifting lug is provided for handling purposes.

Protection against overpressurization of the cask is supplied by means of a pressure relief system. A relief valve set to discharge at 30 psig is connected to the upper portion of the cask cavity. Any material which may be discharged passes through a filter designed to withhold 99.9% of the particles in excess of 0.3 microns in diameter prior to release to the atmosphere. A pressure gauge is also included to provide visual indication of the cask pressure. The relief valve, filter, and pressure gauge are located in a stainless steel enclosure for protective purposes.

A drain system is provided for the cask to permit removal of coolant to obtain an air expansion volume initially and for sampling purposes while in transit. The drain valve is plugged as an added precaution against accidental drainage. The drain valve, like the pressure relief system, is also located within a stainless steel enclosure for protection.

B. Crash Frame

A crash frame consisting of an assembly of H beams as shown in Martin drawing 372-2106016 surrounds the cask. The crash frame is designed to maintain the cask cover in place in the event the cask is subjected to a 30 foot free fall. The frame is constructed of four vertical H beams located symmetrically around the cask circumference and fastened to the cask. Additional framing members placed over the cask cover are mounted to these vertical members to provide a rugged protective assembly.

C. Cask Shroud

A one inch thick steel shroud divided into four segments is placed around the cask to satisfy the total shield requirements as specified by ICC Regulations. This shroud, shown in Martin drawing 372-2106016, is affixed to the cask assembly by bolting to the vertical H beams of the crash frame. A cutout is provided to facilitate access to the drain valve for coolant sampling while in transit. In addition to its shielding function, the shroud also provides additional protection in the event of a free fall.

D. Shipping Pallet

The spent fuel shipping cask, the crash frame, and the shroud are mounted on a shipping pallet to facilitate handling and assure adequate weight distribution in the transport vehicle. The shipping pallet, shown on Martin drawing 372-9010001 Sheet 1 of 3, is constructed of aluminum to minimize weight. Adequate tie-down lugs, designed to withstand 8g loads, are provided to secure the pallet to the transport vehicle.

II. DESCRIPTION OF THE CORE - MECHANICAL DESIGN

A detailed description of the reactor core to be transported is presented in this chapter. The core assembly which is placed in the shipping cask consists of one center and six peripheral bundles contained within a shroud can. Six wye control rods, one in each peripheral bundle, and six supplimentary poison plates, placed between the peripheral bundles, are securely locked in the shroud can along with the fuel bundles by means of a rugged core handling fixture. Each of the above core components is described below.

It is the additional intent of this chapter to demonstrate conclusively that both the control rods and the poison plates can under no accidental conditions be displaced from the core. It is also shown herein that the mechanical design of the core is such that under no circumstances may the core components move relative to each other to obtain a more reactive core geometry.

The following detailed drawings are submitted with this report for additional clarification.

Martin Drawing Number	Title
372 - 2105000	Reactor Assembly
372 - 2105001	Reactor Core Section
372 - 2105002	Installation Reactor Core Structure
372 - 2105003	Center Bundle Assembly
372 - 2105004	Upper Skirt Assembly
372 - 2105005	Core Installation
372 - 2105006	Core Details - Center Bundle
372 - 2105007	Details - Hold Down Center Bundle
372 - 2105009	Core Shroud Assembly
372 - 2105010	Peripheral Bundle

Martin Drawing Number	
372 - 2105011	Upper Grid
372 - 2105012	Lower Grid
372 - 2105013	Core Elements Fuel - Poison - Dummy
372 - 2105014	Control Rod Guide Rails
372 - 2105015	Lock Sleeve & Alignment Structure
372 - 2105016	Control Rod Assembly
372 - 2105017	Spring, Hold Down, Upper Skirt
372 - 2105018	Source (Primary)
372 - 2106000	Core Handling Fixture

A. Core Elements

Three types of core elements are included in each fuel bundle; fuel, poison and dummy. The general construction and dimensions of these elements are shown in Fig. II-1, while their locations within each fuel bundle are given in Fig. II-2 and II-3. These elements have identical end construction to allow complete interchangeability.

The fuel element contains UO_2 dispersed in and clad with stainless steel. Its meat is nominally 0.0285 inch thick and it is sandwiched between cladding of 0.0075 inch thickness. When assembled into a fuel bundle, the active fuel region starts one inch above the top surface of the lower grid. This distance provides length for flow equalization after being orificed by the lower grid and allows the diameter reduction of the tube end to start well away from the fuel dead end interface.

Lumped burnable poison elements are substituted for fuel elements, as required, to provide the desired nuclear characteristics.

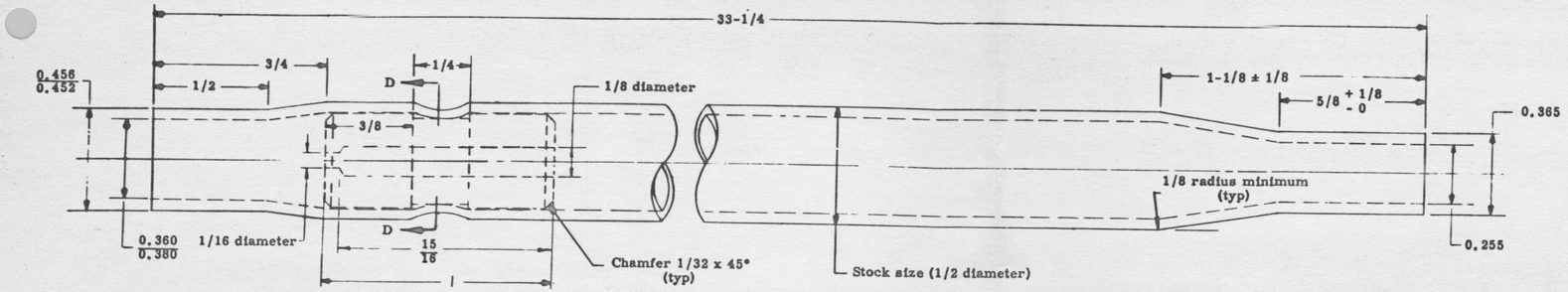

Dummy Element

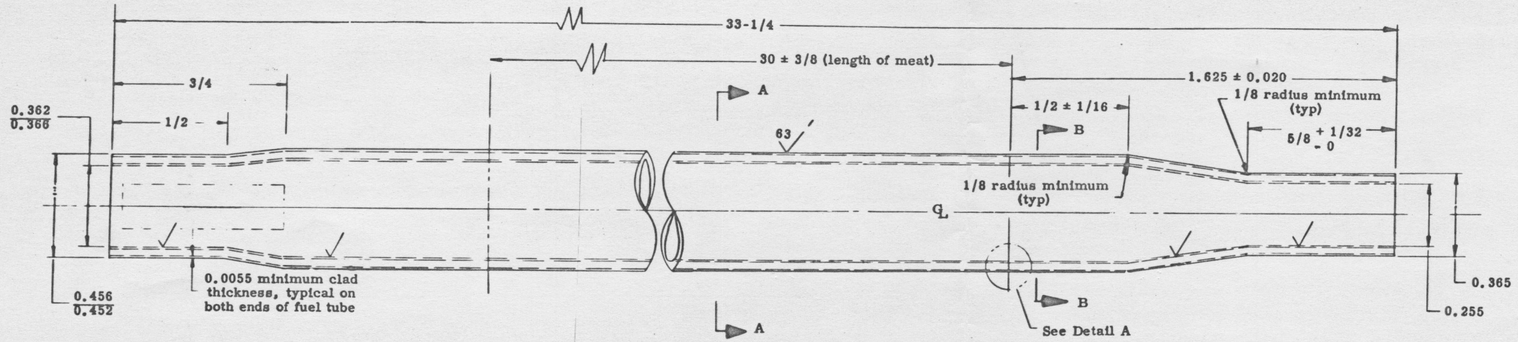

Fuel Element

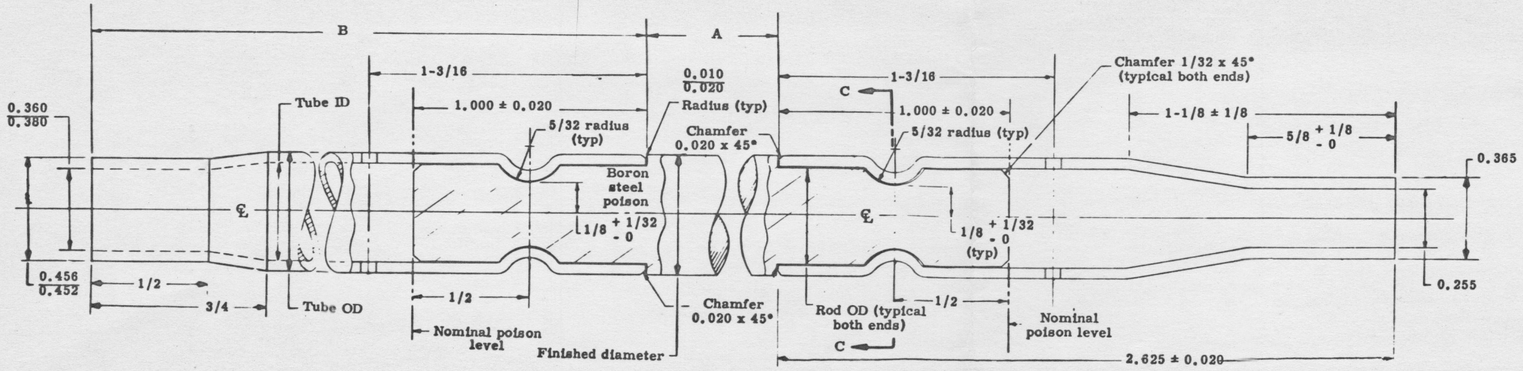

Poison Element

NOTE:
All dimensions in inches.

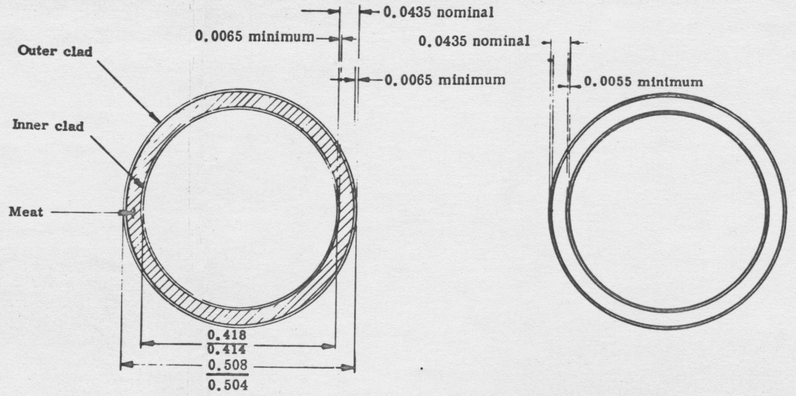

Section A-A

Section B-B
(typical both ends)

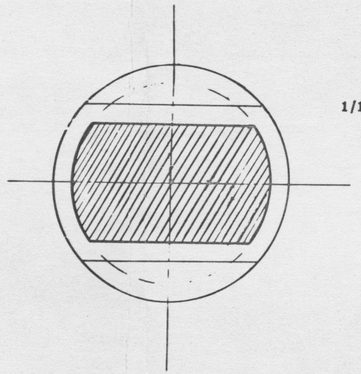

Section C-C

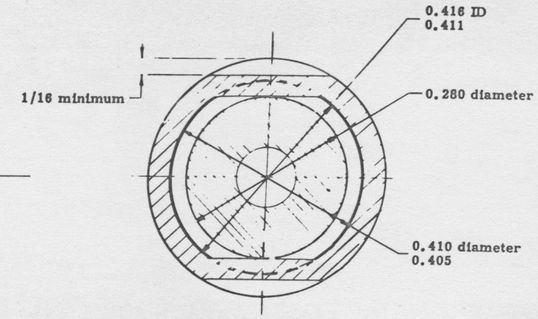

Section D-D

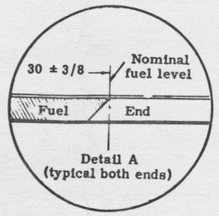

Detail A
(typical both ends)

Dimension Tabulation

	A	B
2/3 length	18.000	
Full length	28.000	
2/3 length		12.625
Full length		2.625

Fig. II-1. Core Elements, Fuel, Poison, Dummy

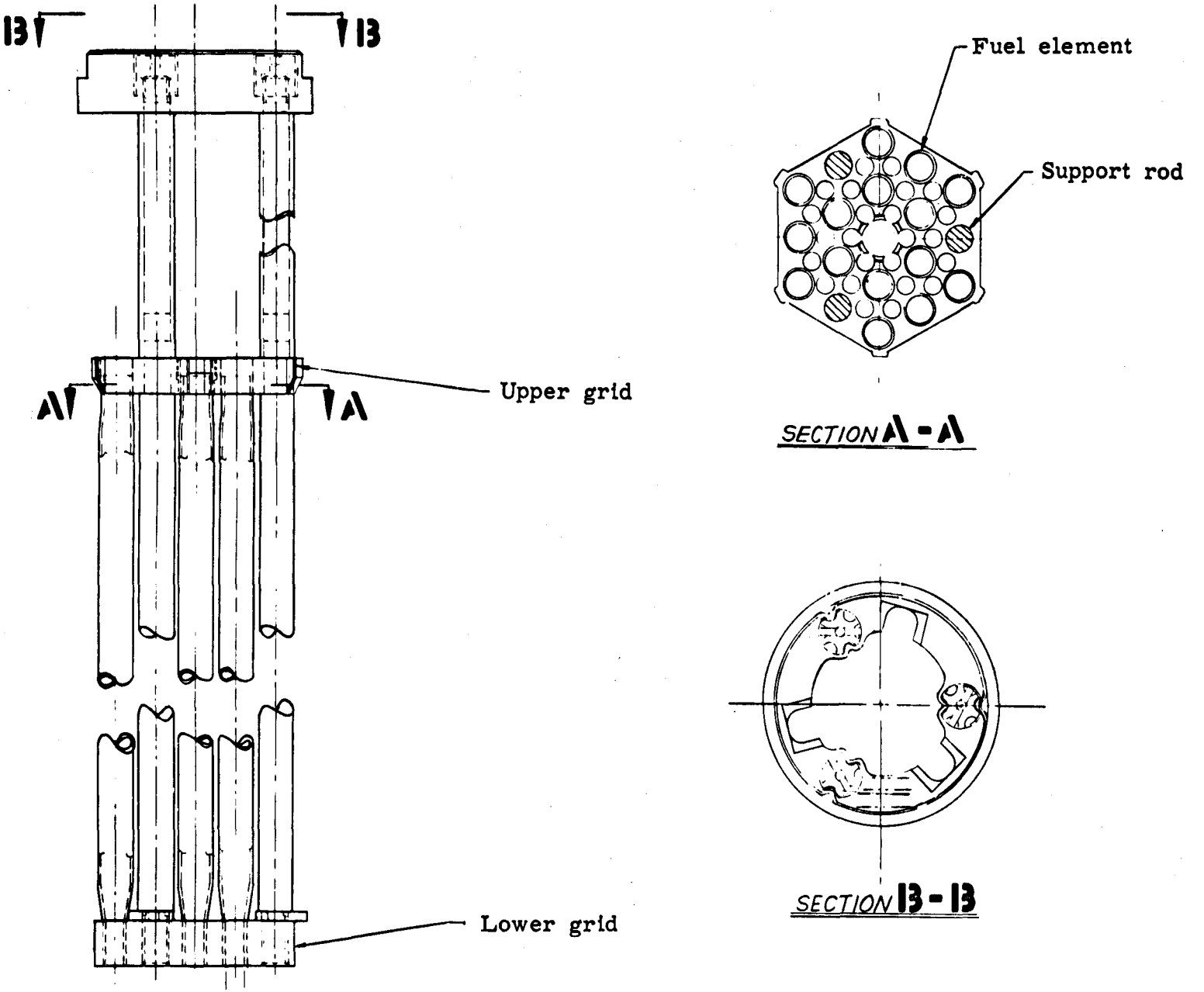

Fig. II-2. Center Bundle Assembly

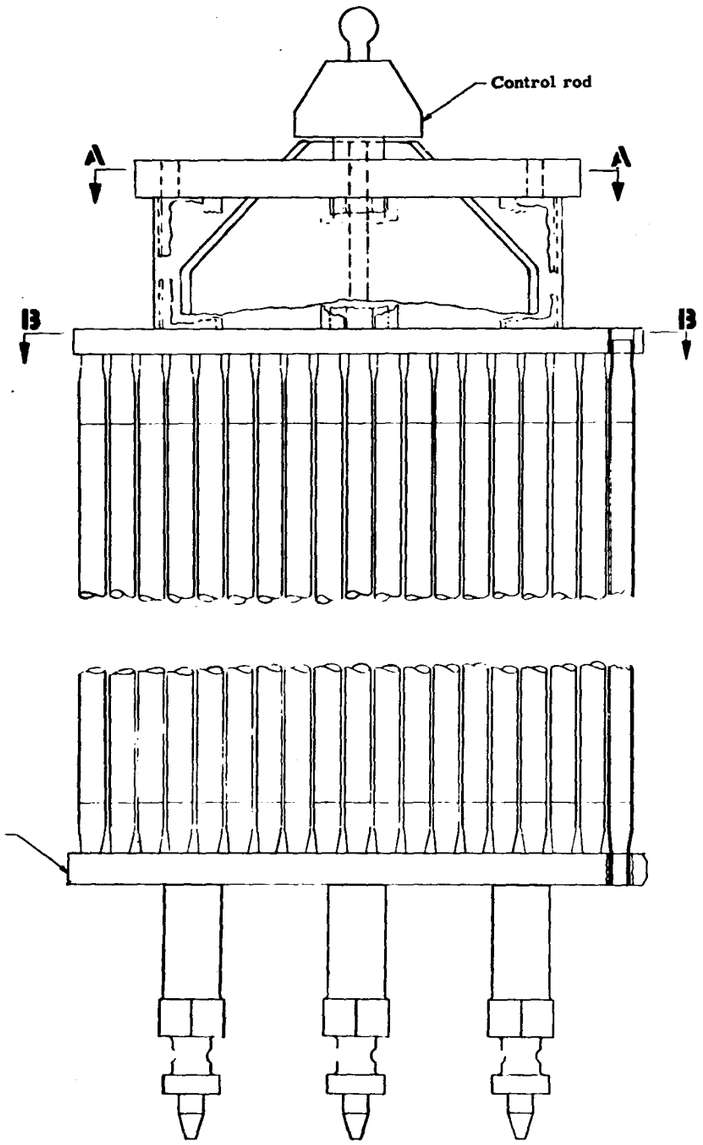

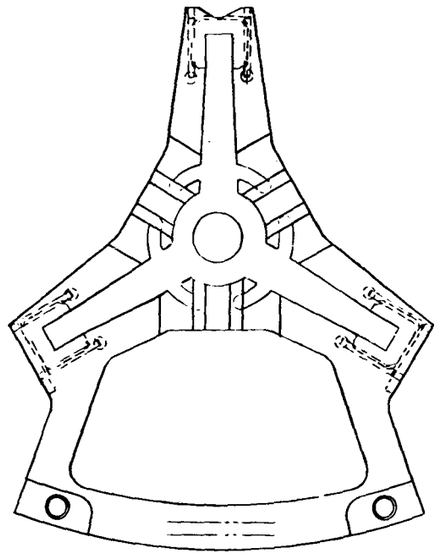

Section A-A

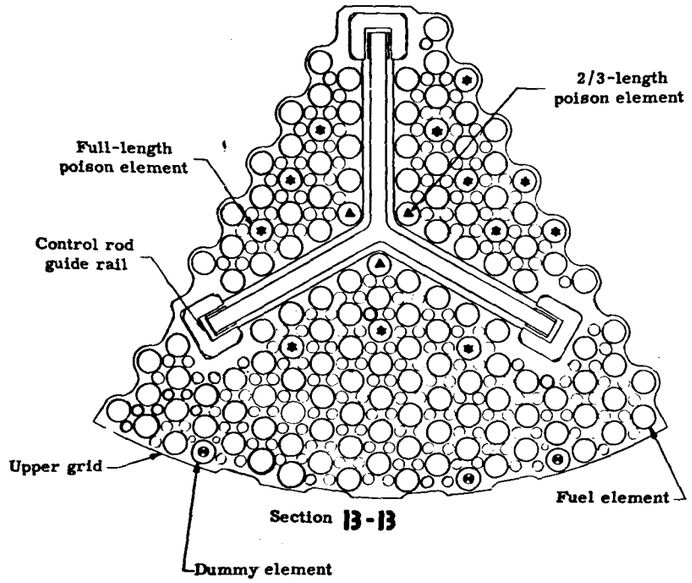

Section B-B

Fig. II-3. Peripheral Bundle Assembly

II-4C

These elements, which are unclad, contain natural boron alloyed in stainless steel. The poison length may be easily varied by the use of unpoisoned "dead ends" which are mechanically fastened and locked to the boron steel section. The poison length was selected to be the same as the fuel length for the full length poison elements. In addition, a number of two-thirds length poison elements are included at the apexes of the control rod blades to satisfy the nuclear requirements. The boron - stainless steel poison elements contain 0.275 w/o boron. As a result of extensive testing, no evidence of any significant corrosion of this alloy, which contains such a relatively small percentage of boron, has been found. Therefore, the poison elements require no cladding protection.

Dummy core elements are incorporated into each peripheral bundle to fill in space at the core periphery where the basic triangular element pattern ends, thus reducing flow requirements. These elements are stainless steel tubes containing plugs to block the flow. These plugs have a small bleed to eliminate the stagnant water area.

B. Fuel Bundles

The active core contained within the shroud consists of seven fuel bundles; one hexagon-shaped center bundle (Fig. II-2) with six identical pie-shaped bundles located around the periphery (Fig. II-3). Each of the peripheral bundles is individually held and positioned within the core shroud as shown in the core installation drawing (372 - 2105002). The center bundle, in turn, rests upon the lower grids of the peripheral bundles and is positioned within their supporting guide rail structure. The fuel element spacing is increased between bundles to allow assembly clearances. As will be discussed, stops are provided to maintain this clearance

at all times during positioning.

Each peripheral bundle is constructed, basically, from three control rod guide rails, an upper and lower grid, a guide alignment structure and the necessary core elements (fuel, poison and dummy). The control rod guides provide the fundamental structural connections for the bundle. They extend over the full length of the assembly and form a continuous track for the control rod wear pads. Positioning of the three guide rails relative to each other is achieved by a fit into the alignment structure at their top and through the lower grid at the bottom. Sleeves thread over the portion of the guide rails which extends through the lower grid to lock it into place. These sleeves provide the seat upon which the bundle rests in the core shroud, as well as the necessary spacing between the grid and shroud alignment spider to provide inlet flow equalization. Each sleeve is mechanically locked into place by deforming its side wall into a corresponding groove. A portion of the turned diameter on the guide rail extends through the sleeve to fit, at assembly, into the positioning holes in the core shroud's alignment spider. Correct upper alignment is achieved through the alignment structure to the two alignment pins located in the core shroud flange. Thus, each control rod guide rail in a peripheral bundle is aligned at its top and bottom, and the complete bundle is allowed free thermal expansion about its seat in the core shroud.

The guide rails fit through cutouts in the upper grid and into the alignment structure. The alignment structure is pinned to the rails and holds the upper grid in place by the use of a spacer and a seat on the rails.

Each guide rail is contoured or, in effect, hollowed out to provide maximum control rod guidance and overall structural rigidity

while minimizing material volume. This was desired to reduce the total nuclear poisoning effect of the stainless steel guides. A wing runs the length of each guide rail within the active core region. This wing interlocks with the guide rail wing in the neighboring fuel bundle to provide bundle spacing and prevent fuel element damage during the insertion or removal of a single bundle from the core shroud.

Each of the core elements is fastened into the lower grid with allowance for free thermal expansion into the upper grid. The connection at the lower grid is achieved by inserting the element into a hole in the grid plate and mechanically expanding it into a counterbore at the lower 1/8 inch of the hole in the grid plate. Both a mechanical bond against the grid wall and an interference fit within the counterbore are obtained in this manner with loads of 700 to 1000 pounds required to free an element. Free axial expansion into the upper grid is provided by a diametrical clearance of 0.002 to 0.008 inch. This clearance suitably restricts any induced vibration but is sufficient to prevent buildup to the extent that it could cause an element to freeze in place.

For proper division of flow between the inside and outside of the fuel tubes, it was necessary to restrict the respective flow areas in the proper ratio. To accomplish this while keeping the exit flow restrictions to a minimum, it is necessary to neck down both ends of each fuel element. Although not required for this reason, all three types of core elements (fuel, poison and dummy) were made with similar end configurations. This allows the use of a single method for fastening the elements into the lower grid. With both ends of an element necked down and located between fixed grid plates, it is completely trapped even if the mechanical connection were improperly made and a failure occurred during operation.

The fuel region of the center bundle is similar to the peripheral bundles. However, support is obtained from tabs which extend at three points from the center bundle lower grid to rest upon the peripheral bundle lower grids. The center bundle is free to expand axially from this point with top radial alignment being obtained by tabs bearing against the peripheral bundle upper grids. Three solid rods extend axially along the length of the center bundle to provide positioning for the pickup plate and the upper and lower grids. Each bar threads into the lower grid, captures the upper grid through the use of a sleeve and secures the pick-up plate into place through the use of a special nut. This nut, which completely locks the assembly, is both encapsulated and prevented from rotating by the positive displacement of its housing into grooves in the nut.

The primary neutron source is located at the middle of the center bundle where a core element has been displaced. Installation of the source into the center bundle will be made just prior to loading the core into the pressure vessel. Because of the relatively low source strength requirements and the ease of assembly, this operation may be performed virtually by hand. The source is simply lowered through the upper grid with radial guidance (but free axial expansion) provided by the lower grid.

C. Control Rods

The control rod (Fig. II-4) utilizes a Y-shaped configuration to fit within the triangular core element pattern. Its poisoned region, consisting of a europium titanate ($Eu_2O_3 \cdot 2Ti\ O_2$) dispersed in stainless steel, is contained within cladding of nominal 0.030 inch thickness.

Each control rod is guided by wear pads on the lower edge of

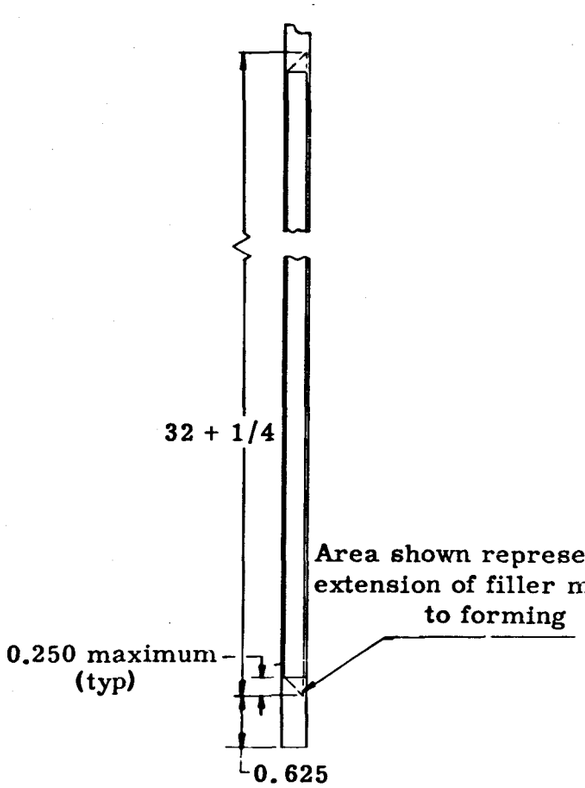

Section B-B

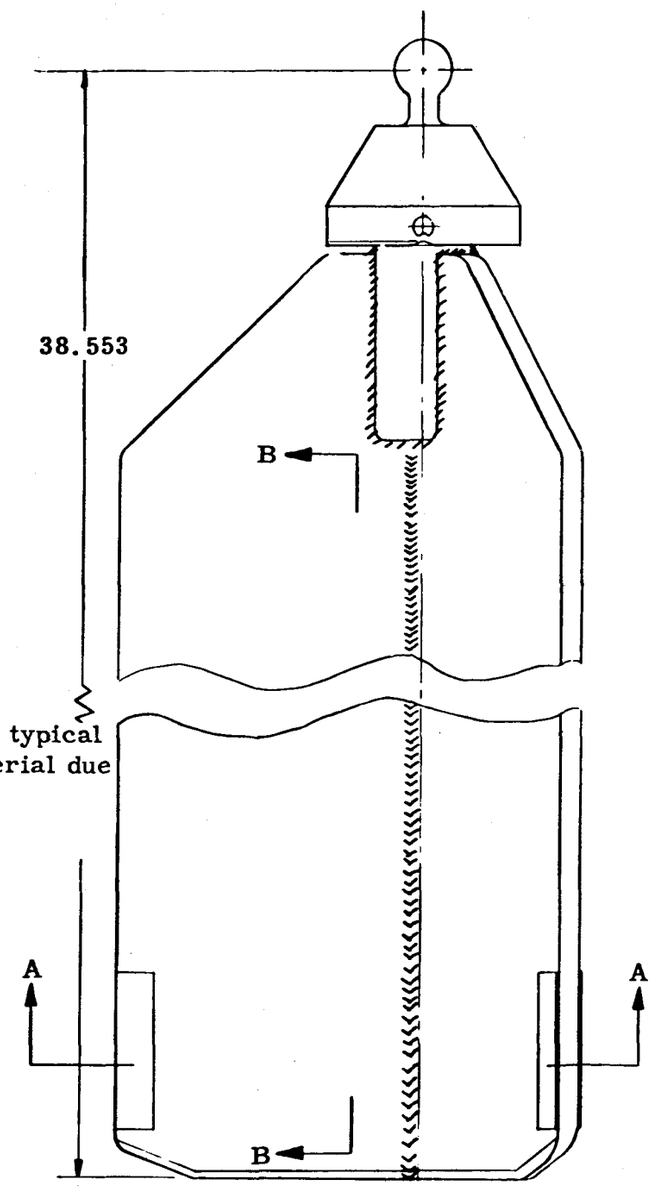

Basic Assembly

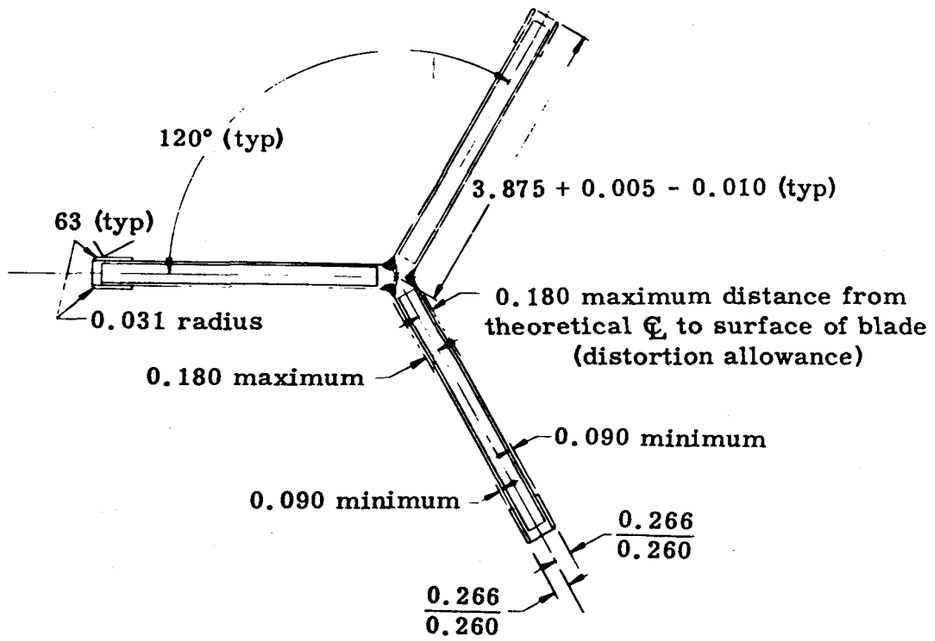

Section A-A

NOTE:
All dimensions in inches

Fig. II-4. Control Rod Assembly

II-64

each blade and a wear ring located at its upper hub. This wear ring also integrally incorporates the pickup ball utilized in latching to the control drive mechanism. The rod wear pads are contained within the three control rod guide rails that run the full length of each peripheral bundle. These pads provide the lower radial and overall angular alignment for the control rod. Upper alignment is obtained through the wear ring, which is located within the guide tube of the upper skirt assembly. This tube, split to allow control rod withdrawal, interlocks with the alignment structure of each peripheral bundle. As discussed previously, the rod guide rails also terminate in this structure, thus providing a continuous structure for control rod guidance as well as overall bundle alignment. Both the wear ring and pads are made from hardened 17-4 pH material to minimize wear between these areas and the guiding structure.

D. Poison Plates

Poison plates, one plate between each peripheral fuel bundle, are installed into the core prior to shipment to guarantee a value of k_{eff} of less than 0.90.

The poison plates are approximately 0.7 $^{w}/_{o}$ natural boron stainless steel alloy corrugated plates which are .062 inches thick. They are inserted into the space between the fuel bundles. The plates are of a corrugated design to conform to the grid design.

The plates have sections attached to the top which will be trapped below the core handling fixture, thus insuring that they cannot become displaced from the core during shipment. As an additional feature, the poison plates extend below the fuel so that the small amount of movement allowed by the core handling fixture will not effect reactivity.

E. Core Shroud

The core shroud, shown in Fig. II-5, is employed both in the shipment and operation of the reactor core. The shroud contains the six peripheral fuel bundles, each with an integral control rod, and one center fuel bundle. The shroud can, in conjunction with the core handling fixture, is completely loaded with fuel bundles and control rods and the entire assembly is shipped as a unit. The design is such that practically no relative movement between the core components can occur.

The core shroud when placed in the reactor pressure vessel rests upon the pressure vessel orifice plate and functions primarily by holding the fuel bundles and positioning them relative to the control drive mechanisms located in the head of the pressure vessel. As secondary functions, it provides the first thermal shield and directs the primary coolant from the pressure vessel orifice plate to the core inlet. An alignment spider is incorporated integrally into the bottom of the shroud. Each of the six peripheral fuel bundles contained within the core rests directly upon this spider. Alignment of the bottom of each bundle is assured through the use of legs which fit into the accurately positioned holes in the spider. Although each bundle sits on three legs, to ease handling during remote assembly, only the two outermost are used for positioning. The centrally located hole is made slightly oversize, providing a seat without accurately controlling the location. Upper bundle positioning is accomplished by the fit of each bundle's alignment structure over two alignment pins located in the top flange of the core shroud. This flange also contains the alignment pins and seat used in positioning the skirt assembly and shroud relative to the orifice plate. Each of these pins is pressed to fit into

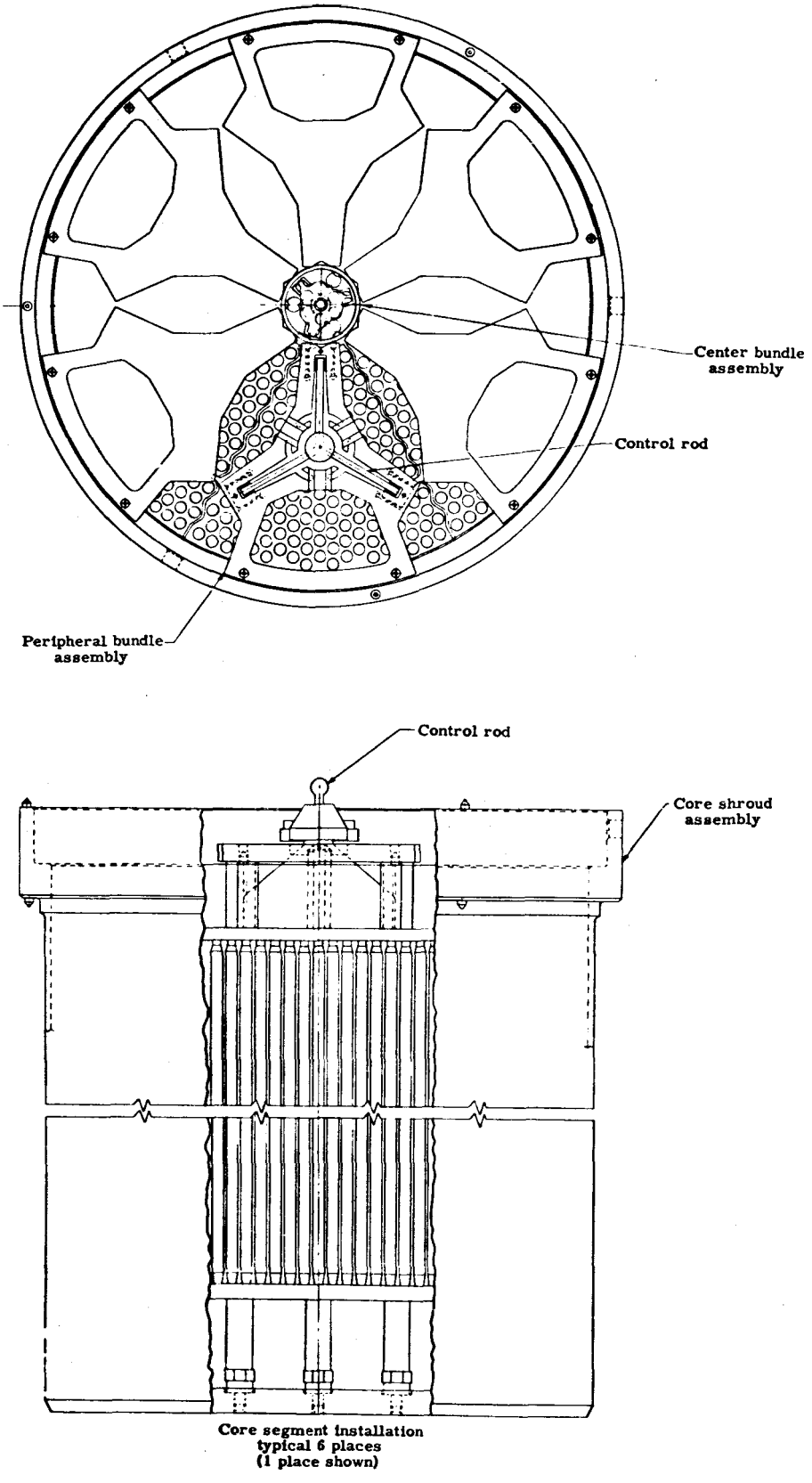

Fig. II-5. Reactor Core Installation

II-8A

place and, in addition, is secured by a smaller lock pin. These lock pins are held mechanically and have their motion limited at assembly by adjoining components. The general arrangement of the reactor-shroud-bundle assembly may be seen in Fig. II-5.

F. Core Handling Fixture

The core handling fixture, shown in drawing 372 - 2106000, is mounted atop the core shroud containing the fuel bundles and control rods whenever the core is handled. When the spent core is placed in the spent fuel shipping cask, additional poison plates described previously are inserted between the peripheral bundles to provide a k_{eff} of less than 0.9. The core handling fixture is then placed in position to lock the fuel bundles, control rods, and poison plates within the core shroud.

The core handling fixture has three rugged lugs which may be inserted into or retracted from their position in the core shroud wall by means of a cam plate. Safety devices on the cam plate assure that the lugs on the handling fixture are locked in either of their extreme positions - completely extended or retracted. When retracted the core cannot possibly be handled with the special tools provided. Only when the lugs are extended into the core shroud wall, thus assuring a unitized assembly, can the core be handled. It is in the latter condition that the spent core is placed into and transported by means of the shipping cask.

The core handling fixture also has integral screw type hold down mechanisms for each peripheral fuel bundle to preclude minor motion or "rattling". These devices are actually tightened against the top of each of the control rods which in turn rest on the tops of the lower grid plates and thereby hold down the peripheral fuel bundles.

Therefore, when the core handling fixture is installed, the core shroud, fuel bundles, control rods, and poison plates essentially become an integral unit which cannot be altered.

G. Conclusions

Based upon the foregoing design description, the following hazards considerations are satisfied:

(1) The fuel bundles, due to their rigid positioning within the core shroud and inherent ruggedness, cannot be rearranged into a more reactive condition.

(2) The control rods and poison plates cannot be displaced from the core under normal or accident conditions to create a hazard during transportation.

H. Appendix

Figures II-6 through II-9 are photographs of the assembly used for the PM-1 gross flow test. Since, the units shown are test assemblies, the photographs show test instrumentation and other variations from an operating reactor core. In general, however, the operating core will be very similar to the assemblies as shown. The photographs are enclosed for illustrative purposes.

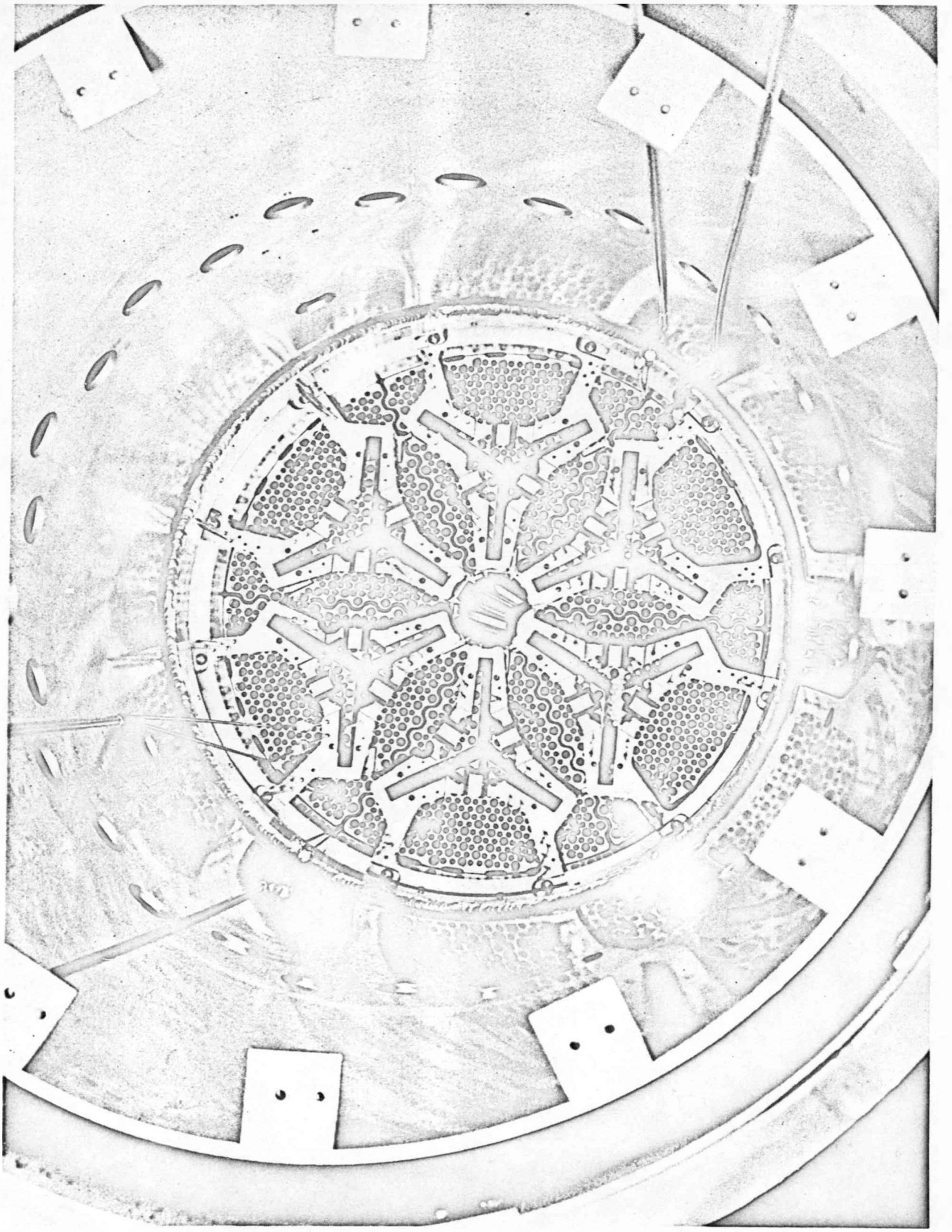

Fig. II-6. Top View of Reactor Core

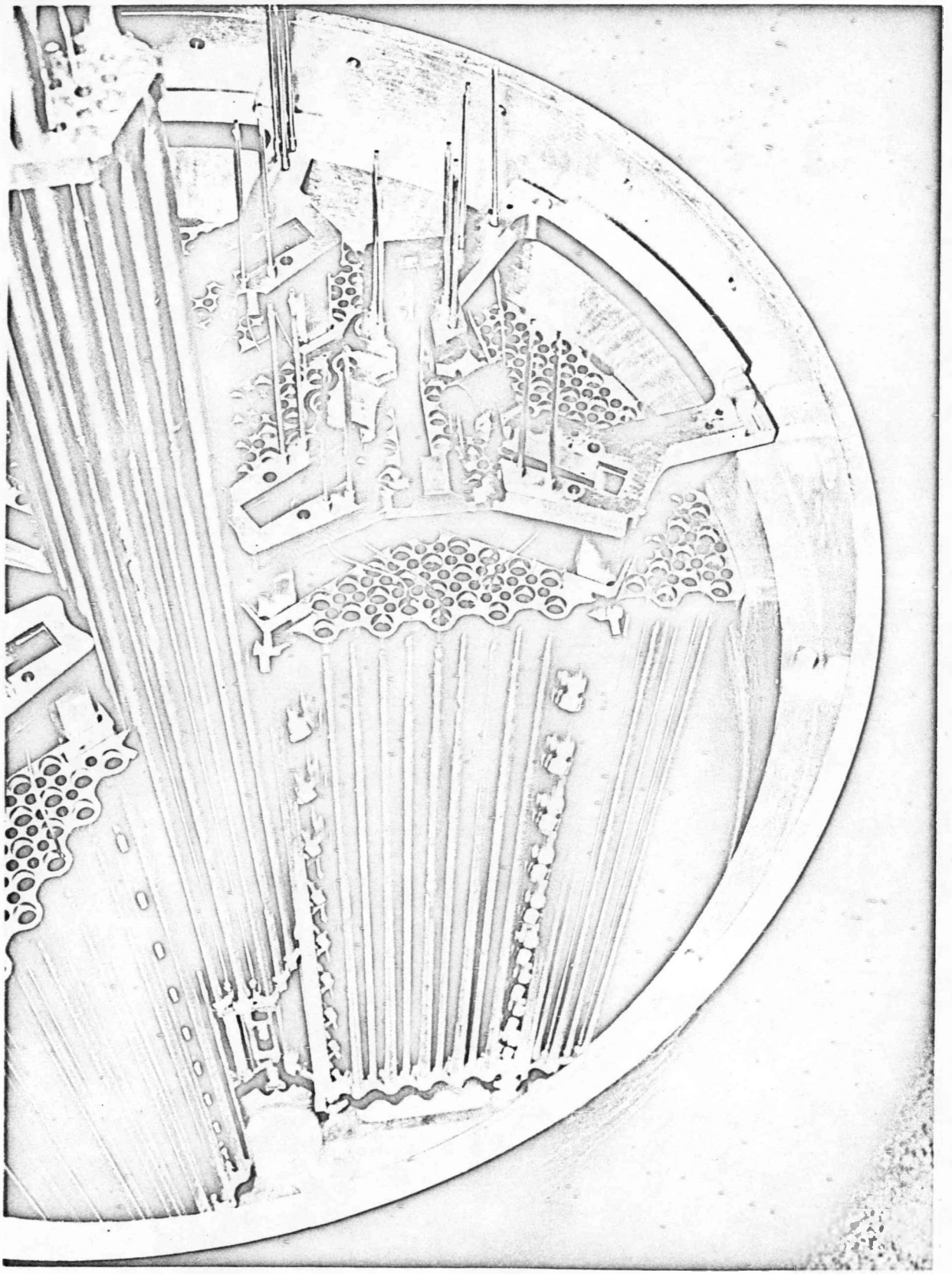

Fig. II-7. View of Reactor Core with Two Peripheral Bundles Removed

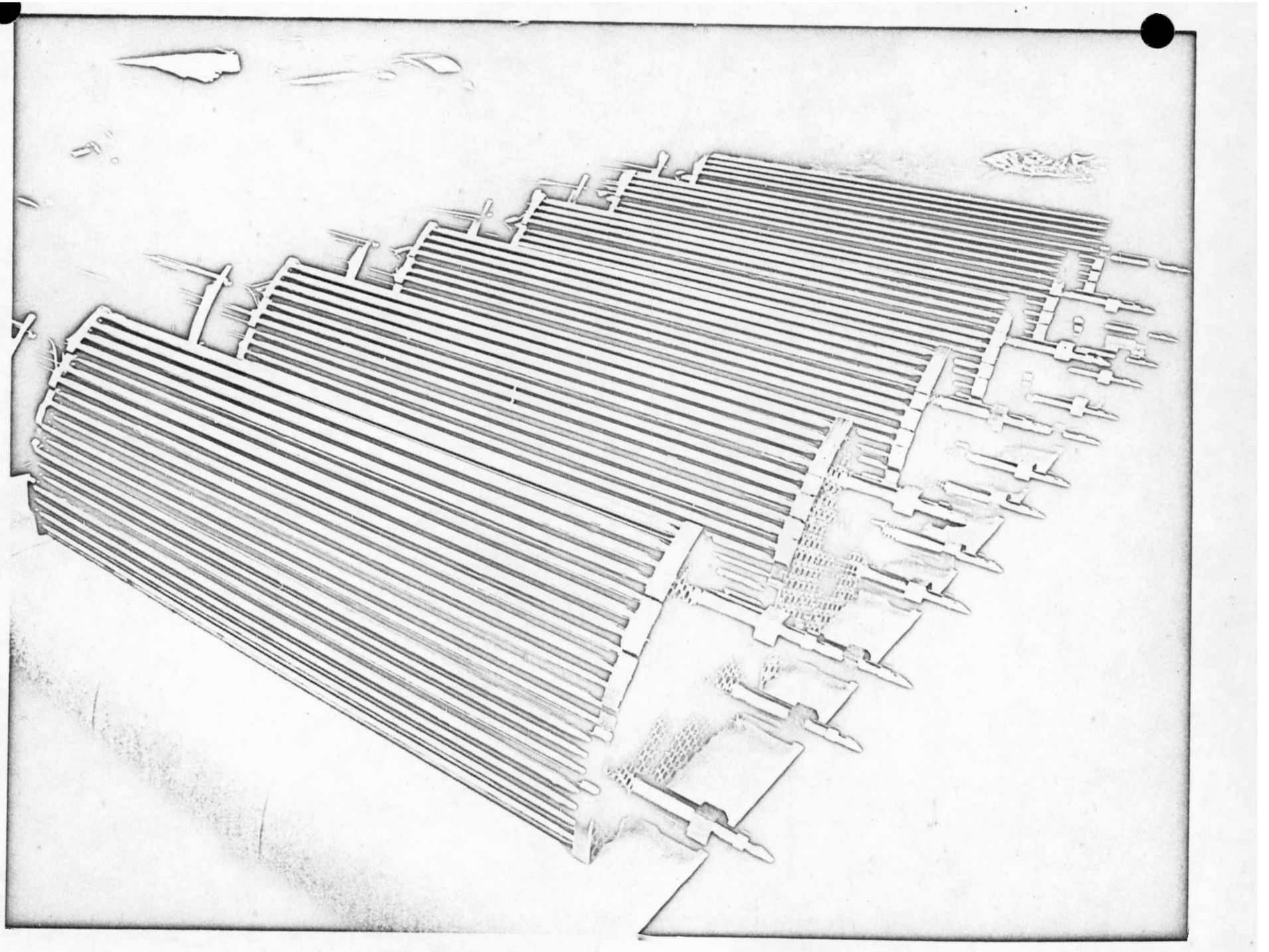

Fig. II-8. View of Peripheral Bundles

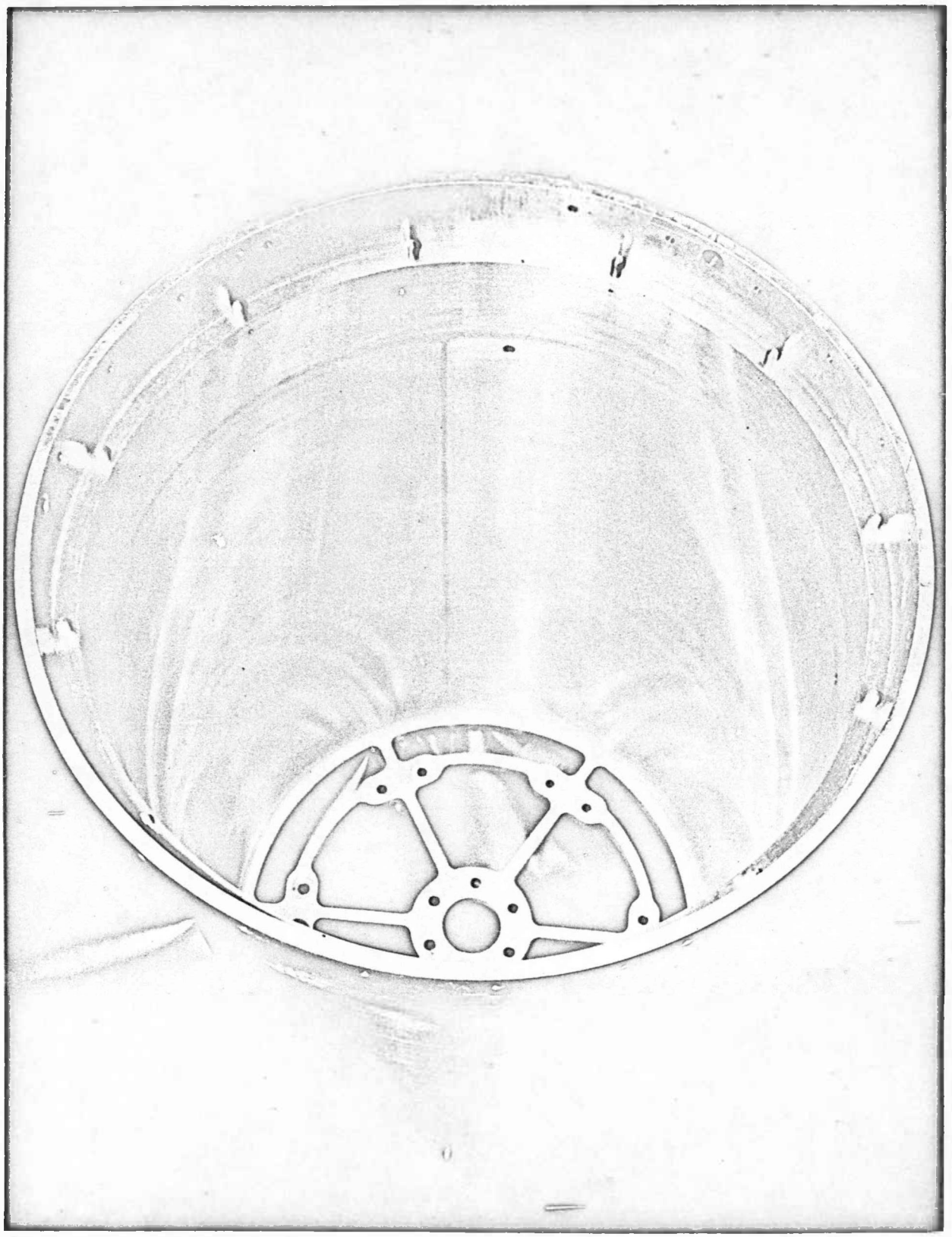

Fig. II-9. View of Core Shroud

Fig. II-10. View of Core Handling Fixture

III. SHIELDING *

It is shown in this section that 7 7/8 inches of lead on the sides of the cask and 8 1/4 inches on the ends will provide adequate shielding so that the gamma dose requirements are met both during shipment by truck and by plane. The unnecessary lead shielding at the outer corners of the cask has been removed to minimize the weight during transit by plane. For shipment by truck, an auxiliary steel shield one-inch thick is placed around the cask.

A. Fuel Element Activity

The gamma activity in disintegrations per second due to the spent core is obtained from reference III-1 as a function of the gamma energies for an irradiation time of two years and a cooling time of one year. The fuel element source strength in roentgens per hour is obtained by multiplying the activity by the energy dependent conversion factor graphed in reference III-2, page 19. This information is listed in Table III-1 for the significant gamma energy groups. The dose due to gammas in groups below 1 Mev is negligible.

TABLE III-1 SPENT CORE ACTIVITY

Energy Group	Average Energy	$A^{(a)}$	$C^{(b)}$	$S^{(c)}$
III	1.35 Mev	9.68×10^{13}	2.45×10^{-6}	2.37×10^{8}
IV	2.5 Mev	4.88×10^{13}	3.75×10^{-6}	1.83×10^{8}

(a) A = activity in $(\frac{dis}{sec})$.

(b) C = energy dependent conversion factor in $(\frac{r}{hr})$ $(\frac{dis}{sec})^{-1}$

* This chapter was prepared for the Edlow Lead Company by Battelle Memorial Institute and submitted to The Martin Company.

(c) S = source strength in $(\frac{r}{hr})$.

B. Dose Calculations

The gamma dose in shielding groups III and IV is calculated using the technique outlined in reference III-2 page 360. According to this development, the dose at a distance d from the side of the cask is,

$$\phi = \tfrac{1}{2} \frac{BS_L}{(t + Z_s + d)} \left[F(\theta_2, b_2) + F(\theta_1, b_2) \right]$$

where

S_L = $S/2\pi L$

L = length of active fuel region

B = dose build-up factor (ref. III-2)

t = $t_{pb} + t_{ss}$

t_{pb} = lead thickness

t_{ss} = steel thickness

d = distance from the shield surface to the point where the dose is calculated

Z_s = self absorption distance of source (ref. III-2)

b_2 = $\mu_{pb} t_{pb} + \mu_{ss} t_{ss} + \mu_s Z_s$

μ = absorption coefficients (cm^{-1})

$$\theta_1 = \tan^{-1}\left[\frac{\frac{L}{2} - h}{t + Z_s + d} \right]$$

$$\theta_2 = \tan^{-1}\left[\frac{h + \frac{L}{2}}{t + Z_s + d} \right]$$

h = distance above midplane of cask

$$F(\theta_1 b_2) = \int_0^{\theta} e^{-b_2 \sec \theta'} d\theta' \quad \text{(ref. III-2)}$$

The volume fractions of uranium, steel, and water in the cavity are:

$f_{UO_2} = .00982$

$f_{ss} = .322$

$f_{H_2O} = .678$

Knowing the volume fractions of the constituents, the absorption coefficient "μ_s" is calculated by homogenizing the material inside the cask cavity. The absorption coefficients used in the calculations to follow are listed in Table III-2.

TABLE III-2 ABSORPTION COEFFICIENTS

Group	μ_{H_2O}	μ_{ss}	μ_{UO_2}	μ_{pb}	μ_s
III	.061	.483	.609	.642	.173
IV	.044	.348	.438	.474	.129

C. Gamma Dose (Truck Shipment)

The gamma dose requirements during shipment by truck are less than 200 mr/hr at the cask surface and less than 10 mr/hr at one meter from the cask. During shipment by truck, an auxiliary steel shield one-inch thick is placed around the cask 6 inches from the cask surface.

The maximum gamma dose ($\theta_1 = \theta_2$) at one meter with a lead shield thickness of 7 7/8 inches and an auxiliary steel shield thickness of 1.0 inch is calculated below. The parameters are listed in a tabular

form convenient for calculation. The total thickness of the steel encasing the lead is t_{ss} = 3/4 inch.

TABLE III-3

Group	b_{pb}	B	b_2	t + Z + d	$\theta_1 = \theta_2$
III	13.1	5.1	16.86	152.0	14.1°
IV	9.67	4.8	12.70	153.3	13.96

Group	S_L	$F(\theta_1 b_2)$	ϕ
III	4.94×10^5	9.5×10^{-9}	$.158 \times 10^{-3}$
IV	3.82×10^5	6.7×10^{-7}	7.90×10^{-3}

Note that d = 1 meter + 6 inches in the calculations above. From the last column, the total dose at one meter is ϕ = .158 + 7.90 = 8.06 mr/hr, which is less than the permissible 10 mr/hr at one meter.

The dose at the surface of the cask without the one-inch auxiliary steel shield is calculated in the next section where the shielding for air shipment is considered. It is shown there that the dose at the outer edge of the 3.0-inch fins is about 100 mr/hr, so that the shielding will certainly be adequate for truck shipment when the one-inch steel shield is in place.

D. Gamma Dose (Air Shipment)

The gamma dose requirements during shipment by plane are less than 200 mr/hr at the outer edge of the 3.0-inch fins and less than 10 mr/hr at 3 meters from the cask. The unnecessary lead shielding at the corners of the cask has been removed to meet the airplane

TABLE III-5 SURFACE DOSE

Group	b_{pb}	B	b_2	$t + Z_s + d$	$\frac{BS_L}{2(t + Z + d)}$
III	12.31	4.8	15.11	38.31	3.12×10^4
IV	9.07	4.8	11.34	39.66	2.31×10^4

Group	h	θ_1	θ_2	$F(\theta_2, b_2)$	$F(\theta_1, b_2)$	ϕ
III	0	44.0°	44.9°	8.5×10^{-8}	8.5×10^{-8}	5.31
IV	0	43.8°	43.8°	4×10^{-6}	4×10^{-6}	$\frac{185}{190.3 \frac{mr}{hr}}$

Group	h	θ_1	θ_2	$F(\theta_2, b_2)$	$F(\theta_1, b_2)$	ϕ
III	10"	18.33	58.9	8.5×10^{-8}	6.9×10^{-8}	4.81
IV	10"	17.75	58	4×10^{-6}	3×10^{-6}	$\frac{162}{167 \frac{mr}{hr}}$

Group	h	θ_1	θ_2	$F(\theta_2, b_2)$	$F(\theta_1, b_2)$	ϕ
III	15"	0	~ 60	8.5×10^{-8}	0	2.65
IV	15"	0	~ 60	4×10^{-6}	0	$\frac{92.5}{95.2 \frac{mr}{hr}}$

Group	h	θ_1	θ_2	$F(\theta_2, b_2)$	$F(\theta_1, b_2)$	ϕ
III	20"	18.33°	~65	8.5×10^{-8}	-6.9×10^{-8}	0.5
IV	20"	17.75°	~65	4×10^{-6}	-3×10^{-6}	$\frac{23.1}{23.6 \frac{mr}{hr}}$

Group	h	θ_1	θ_2	$b_{sec}\theta_2$	ΔF	ϕ
III	30"	44.9	71.45	21.3		
IV	30"	43.8	70.85	15.78	1.05×10^{-8}	$\frac{0.24}{\phi < 0.24 \frac{mr}{hr}}$

For h = 30 inches, an upper limit was placed on $\Delta F(\theta, b_2)$ by using the definition of $F(\theta, b_2)$. Thus,

$$\Delta F = F(\theta_2, b_2) - F(\theta_1, b_2) = \int_{\theta_1}^{\theta_2} e^{-b_2 \sec\theta} d\theta$$

$$\int_{\theta_1}^{\theta_2} e^{-b_2 \sec\theta_2} d\theta = e^{-b_2 \sec\theta_2} (\theta_2 - \theta_1).$$

For group IV, $\Delta F < e^{-15.78} \left(\frac{70.85 - 43.8}{360}\right) = 1.05 \times 10^{-8}$

The results of the calculations in Table III-5 and the results of a similar calculation for another lead thickness are shown in Fig III-1 as a plot of surface dose versus lead thickness as a function of axial distance from the midplane of the cask. Fig. III-1 has been used to construct Fig. III-2 which is a plot of the cask height versus the lead thickness required to make the outer edge of the fins a 100 mr/hr isodose surface, providing a dose safety factor or two. Fig III-2 also shows the amount of lead removed in the final design. Note that the full active fueled length of 30 inches is shielded by 7 7/8 inches of lead and that 5.0 inches have been removed from the cask radius at the ends of the cask.

E. End Dose

The gamma dose at the ends of the cask must be less than 200 mr/hr at the surface and less than 10 mr/hr at 1 meter. A conservative estimate of the dose at the top of the cask is calculated according to reference III-2, p.364, as

$$\phi = \frac{BS_v}{2\mu_s} \left[E_2(b_1) - \frac{E_2(b_1 \sec\theta_1)}{\sec\theta_1} \right]$$

where $S_v = \frac{S}{\pi R_1^2 L}$ = source strength per cm^3 (Table III-1)

R_1 = inside radius of cask = 12 inches

$b_1 = \mu_{pb} t_{pb} + \mu_{ss} t_{ss}$

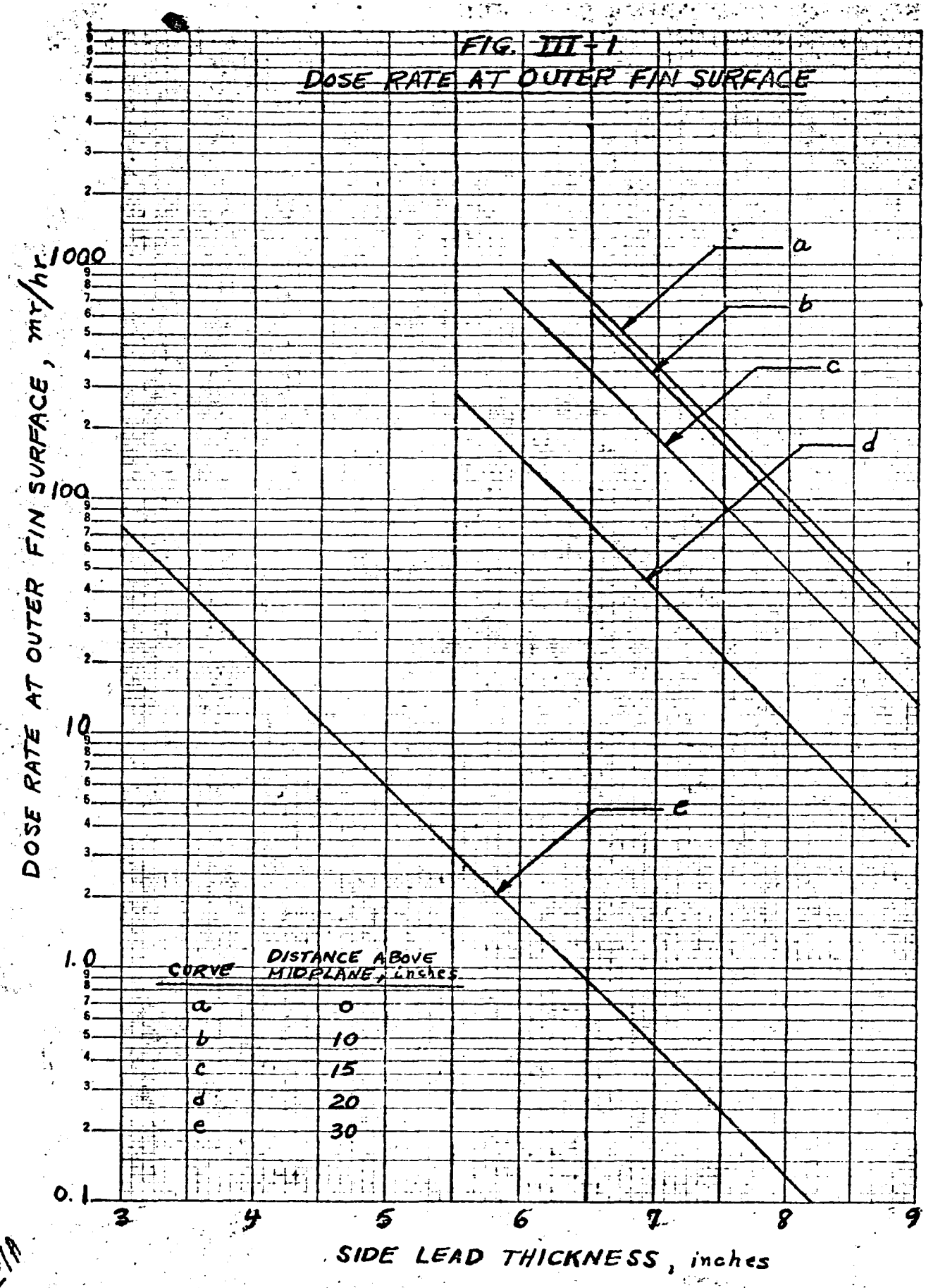
FIG. III-1
DOSE RATE AT OUTER FIN SURFACE
DOSE RATE AT OUTER FIN SURFACE, mr/hr
1000
100
10
1.0
0.1
3
4
5
6
7
8
9
SIDE LEAD THICKNESS, inches
a
b
c
d
e
CURVE
DISTANCE ABOVE MIDPLANE, inches
a 0
b 10
c 15
d 20
e 30

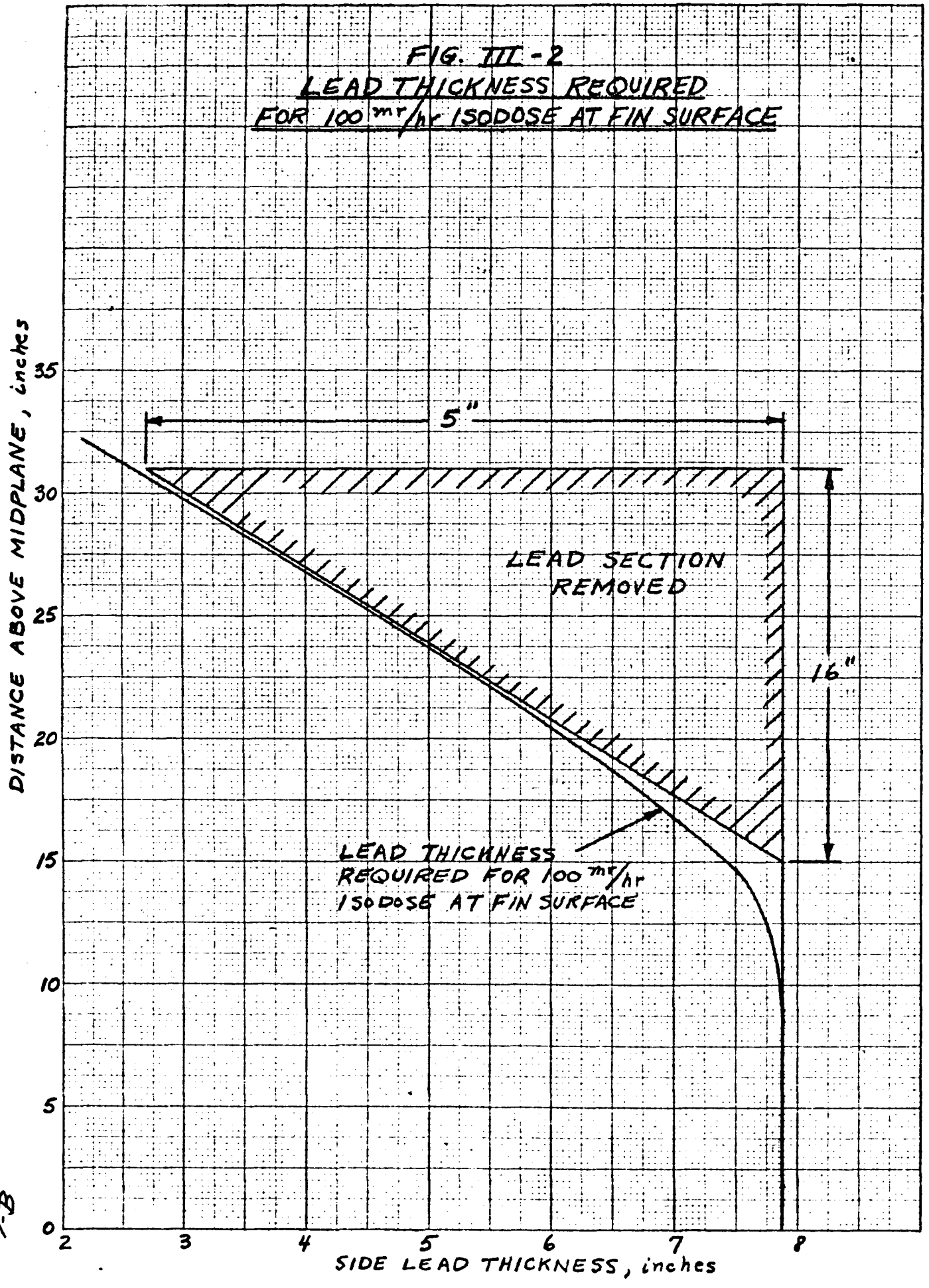
FIG. III-2
LEAD THICKNESS REQUIRED
FOR 100 mr/hr ISODOSE AT FIN SURFACE
DISTANCE ABOVE MIDPLANE, inches
SIDE LEAD THICKNESS, inches
5"
16"
LEAD SECTION REMOVED
LEAD THICKNESS REQUIRED FOR 100 mr/hr ISODOSE AT FIN SURFACE
0
5
10
15
20
25
30
35
2
3
4
5
6
7
8

III-3

$$E_2(b) = b \int_b^{\infty} e^{-x} \frac{dx}{x^2}$$

$$\theta_1 = \tan^{-1} \frac{R_1}{t + d_o + d}$$

d_o = distance from top of active fuel region to top of cask cavity = 15.25/2 inches

The dose at 1 meter for the final design lead thickness of 8 1/4 inches and the surface dose are calculated in Table III-6. The angle θ_1 is

$$\theta_1 = \tan^{-1} \frac{30.5}{42.74\ d}$$

where

R_1 = 12 inches = 30.5 cm

t_{pb} = 8.25 inches

t_{ss} = 1 inch

d_o = 7.625 inches

} 42.74 cm

TABLE III-6 END DOSE

Group	b_{pb}	B	b_1	$10^{-3}\ S_v$	μ_s	$\frac{BS_v}{2\mu_s}$
III	13.45	5.2	14.43	1.066	.173	1.61×10^4
IV	9.82	5.1	10.62	.824	.129	1.628×10^4
			d = 1 meter, sec θ_1 = 1.0227			

TABLE III-6 END DOSE (continued)

Group	$b_1 \sec \theta_1$	$E_2(b_1)$	$\frac{E_2(b_1 \sec \theta_1)}{\sec \theta_1}$	ϕ
III	14.78	3.4×10^{-8}	2.25×10^{-8}	$.185 \times 10^{-3}$
IV	10.87	2.1×10^{-6}	1.565×10^{-6}	$\frac{8.7 \times 10^{-3}}{8.9 \frac{mr}{hr}}$
		$d = 0$, $\sec \theta_1 = 1.23$		
Group	$b_1 \sec \theta_1$	$E_2(b_1)$	$\frac{E_2(b_1 \sec \theta_1)}{\sec \theta_1}$	ϕ
III	17.72	3.4×10^{-8}	$.812 \times 10^{-9}$	$.535 \times 10^{-3}$
IV	12.08	2.1×10^{-6}	1.14×10^{-7}	$\frac{32.6 \times 10^{-3}}{33 \frac{mr}{hr}}$

From the last column in Table III-6, the total doses are 8.9 mr/hr at one meter and 33 mr/hr at the cask surface.

IV. CRITICALITY CONSIDERATIONS

A nuclear analysis was performed to evaluate:

1.) the k_{eff} of the fresh, full core including control rods while in the shipping cask, and

2.) the poisoning required, if any, to lower the k_{eff} to a value of 0.90.

The results of the fresh core analysis showed that k_{eff} for the core in the design cask is 0.921.

An analysis was made to determine the effect of adding boron to the inner stainless steel liner of the cask. The results were unsatisfactory; the addition of 2 w/o B-10 reduced k_{eff} to 0.913.

The addition of a neutron poison inserted into the core was then considered. The poison element selected is a natural boron - stainless steel sheet 1/16" thick. The sheet takes an approximate sine-wave form and is placed in the 0.110 inch slot between the peripheral bundles of the core. A total of 6 such elements are used. They enter radially from the center of the core and are located in the 2 to 8½ inch radial segment as shown in Fig. IV-1. The elements extend greater than the full length of the core.

The results of the analysis show that these poison elements containing 0.7 weight percent natural boron will lower k_{eff} to below 0.895. The details of the analysis are given in the following section.

A. Description of the Analysis

k_{eff} was determined by a three group, radial, multiregion diffusion code, program F3 (Ref. IV-1). The geometry consists of a

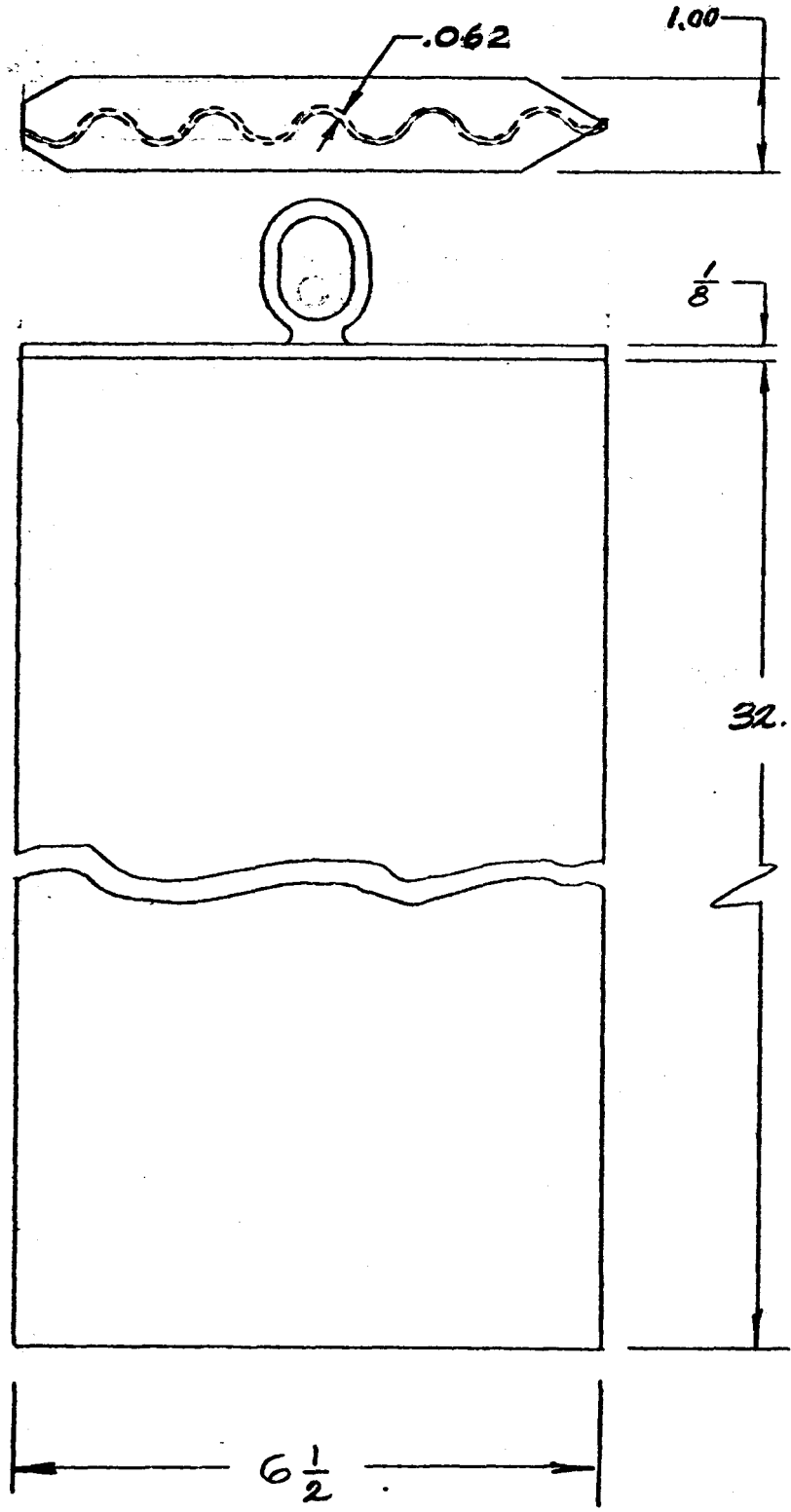

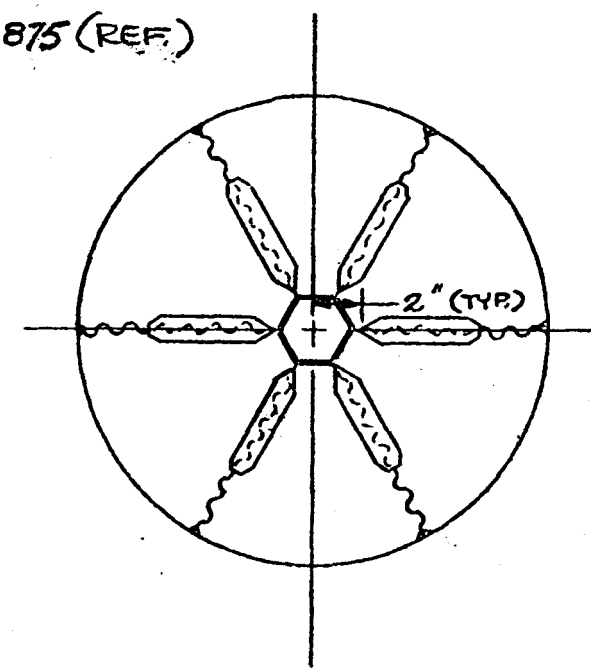

FIG. IV - 1

POISON ELEMENT DESIGN AND LOCATION WITHIN CORE

IV.1-A

one region core surrounded by water, shroud can, and 5 cask regions. Boron-10/stainless steel lumped poison rods were assumed to be uniformly distributed in the core, and the reactivity calculation was repeated for several values of boron-10 concentration. Thermal and epithermal self-shielding factors were obtained from a previous study (Ref. IV-2). From the reactivity calculations k_{eff} was determined as a function of the thermal neutron absorption due to the added poison. This relationship is shown in Fig. IV-2. The thermal neutron absorption is given by:

$$f_{th} \left(N_{B-10} \sigma_a^{B-10} + N_{SS} \sigma_a^{SS} \right) \bar{\phi}_c \qquad (1)$$

where:

f_{th} = thermal self-shielding factor

N_{B-10} = atom density of B-10

N_{SS} = atom density of SS

σ_a^{B-10} = thermal absorption cross section of B-10

σ_a^{SS} = thermal absorption cross section of stainless steel

$\bar{\phi}_c$ = average core thermal flux

The value of the above absorption corresponding conservatively to $k_{eff} = 0.895$ was set equal to the thermal neutron absorption of the design poison elements, which is given by:

$$f'_{th} \; N'_{B-10} \; \sigma_a^{B-10} \; \bar{\phi}_c \qquad (2)$$

where the prime denotes the design poison element. The absorption due to stainless steel was neglected providing an additional margin

IV-2A

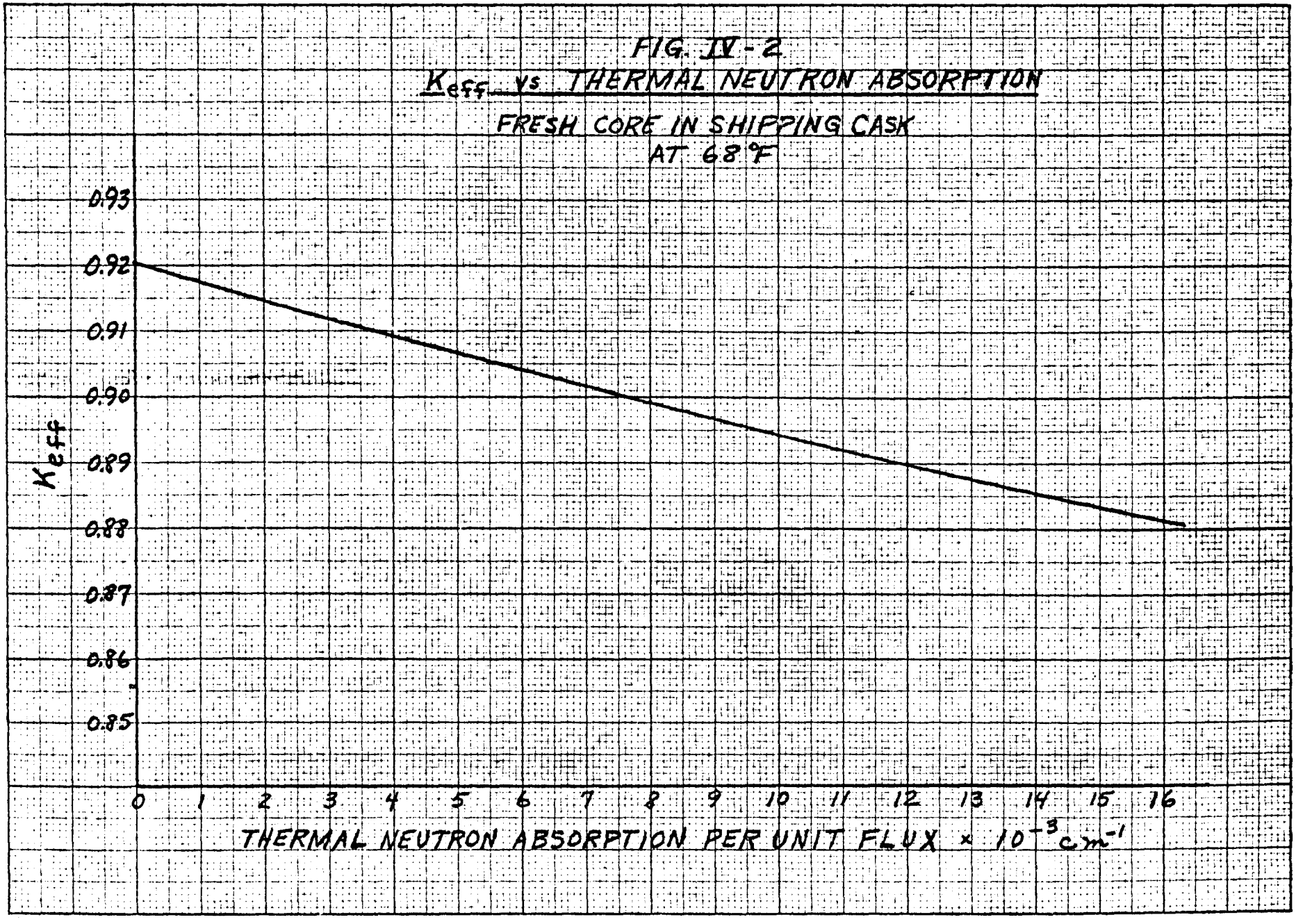
FIG. IV-2
K_{eff} vs THERMAL NEUTRON ABSORPTION
FRESH CORE IN SHIPPING CASK
AT 68°F
0.93
0.92
0.91
0.90
0.89
0.88
0.87
0.86
0.85
K_{eff}
0 1 2 3 4 5 6 7 8 9 10 11 12 13 14 15 16
THERMAL NEUTRON ABSORPTION PER UNIT FLUX × 10^{-3} cm^{-1}

of conservatism. The resulting equation was solved for f'_{th} as a function of N_{B-10}, other quantities being known. This function is shown in Fig. IV-3, where N_{B-10} is given in terms of weight percent of natural boron. The curve defines those combinations of weight percent natural boron and self-shielding factor for the design poison elements which will lower the k_{eff} of the core to below 0.895. For a given weight percent natural boron values of the self-shielding factor which lie above the curve correspond to to values of k_{eff} less than 0.895.

A design poison element containing 0.7 weight percent natural boron was selected, and the thermal self-shielding factor was determined by a one group transport calculation (Ref. IV-3). The calculation assumed a slab geometry with the poison element surrounded by a homogenized core region. The calculated value is 0.526. It is seen from Fig. IV-3 that this value exceeds that required, i.e., the 0.7 weight percent poison element is more than adequate to provide a k_{eff} below 0.895.

V. HEAT TRANSFER - WATER COOLANT PRESENT*

This section of the report demonstrates the heat transfer capabilities of the cask. The cask is designed to remove 2KW of decay heat from the spent core with water coolant present. The rate of decay heat released from the spent core is shown in Fig. V-1.

A. Heat Transfer Inside Cask

The heat transfer inside the cask is calculated in this section. The fuel elements are cooled by water circulating by natural convection up through the fuel elements and down a 3/8 in. annulus around the inside perimeter of the cask. The fluid flow and heat transfer are described below by integrating Bernoulli's equation around a flow loop and performing heat balances over the fuel elements and cask wall.

1. Development of Heat Transfer Equations - Consider first the Bernoulli equation for the system in differential form

$$\frac{-dP}{\rho} = dZ + \frac{VdV}{g} + dF \qquad (1)$$

where the notation is defined in Table V-1.

If the equation above is multiplied by ρ and integrated around a complete circuit and the kinetic energy term is neglected, the following equation results:**

$$-\oint dP = 0 = \oint \rho dZ + \oint \rho dF$$

or

$$-\oint \rho dZ = \oint \rho dF \qquad (2)$$

* This chapter was prepared for The Edlow Lead Company by Battelle Memorial Institute and submitted to the Martin Company.

** See Table V-1 for nomenclature

FIG V-1

TOTAL ENERGY RELEASE RATE FROM DECAY OF FISSION PRODUCTS ASSUMING CONTINUOUS CORE OPERATION FOR 2 YEARS AT 10 MEGAWATTS

TOTAL ENERGY RELEASE, Kilowatts

SPENT CORE DECAY HEAT

ONE YEAR DECAY PERIOD

TIME AFTER CORE SHUTDOWN, seconds

Letting $\rho = \bar{\rho}(1 - \beta T)$, this becomes

$$\bar{\rho}\beta(\bar{T}_i - \bar{T}_o)L = \oint \rho \, dF \ , \qquad (3)$$

where $\bar{T}_i = \int_o^L \frac{T_i(Z)dZ}{L}$ and $\bar{T}_o = \int_o^L \frac{T_o(Z)dZ}{L}$

Equation (3) is the flow equation which must be satisfied. In addition, the continuity equation must be satisfied,

$$V_i A_i = V_o A_o \qquad (4)$$

The heat balance equations must now be considered. Since the velocity and heat production are uniform in the fuel elements,

$$T(L) = T(0) + \frac{Q}{Cp\bar{\rho}V_i A_i} = T(0) + \gamma \qquad (5)$$

and

$$\bar{T}_i = \frac{T(L) + T(0)}{2} \qquad (6)$$

In the outside flow annulus, the following equation is satisfied:

$$\frac{dT(Z)}{dZ} - \frac{h_e P_o^H T(Z)}{Cp\bar{\rho}V_o A_o} = \frac{h_e P_o^H T_o}{Cp\bar{\rho}V_o A_o}$$

Thus,

$$T(Z) = \left[T(L) - T_o\right] e^{-\alpha(L-Z)} + T_o \qquad (7)$$

where $\alpha = \frac{h_o P_o^H}{Cp\rho V_o A_o}$

Equations (3), (5), (6), and (7) can now be used to obtain

$$T(0) = T_o + \frac{\gamma e^{-\alpha L}}{1 - e^{-\alpha L}} \qquad (8)$$

$$T(L) = T_o + \frac{\gamma}{1 - e^{-\alpha L}} \qquad (9)$$

$$\bar{T}_o = T_\bullet + \frac{\gamma}{\alpha L} \tag{10}$$

$$\bar{T}_i = T_o + \frac{1}{2}\alpha\left(\frac{1 + e^{-\alpha L}}{1 - e^{-\alpha L}}\right) \tag{11}$$

Finally using (10) and (11) in (3),

$$\rho\beta\gamma L\left[\frac{1}{2}\left(\frac{1 + e^{-\alpha L}}{1 - e^{-\alpha L}}\right) - \frac{1}{2L}\right] = \oint \rho\, dF \tag{12}$$

Neglecting end losses, the friction pressure drop term becomes

$$\oint \rho\, dF = 4f_i\left(\frac{L}{D_i}\right)\rho\frac{V_i^2}{2g} + 4f_o\left(\frac{L}{D_o}\right)\rho\frac{V_o^2}{2g} \tag{13}$$

For large αL, the term in the square brackets of equation (12) simplifies to $\frac{\alpha L}{12}$. Using this simplification equation (12) becomes

$$\rho\beta\gamma L\left(\frac{\alpha L}{12}\right) = 4f_i\left(\frac{L}{D_i}\right)\rho\frac{V_i^2}{2g} + 4f_o\left(\frac{L}{D_o}\right)\rho\frac{V_o^2}{2g} \tag{14}$$

Using the heat transfer and friction factor correlations, equation (14) can be solved for V_o or V_i. Knowing the velocities, the temperatures can then be calculated.

TABLE V-1 - HEAT TRANSFER NOMENCLATURE

Q	= Total average axial power in $\frac{BTU}{hr}$
Z	= Axial distance from bottom of fuel element, ft
T_o	= Temperature of lead cask wall, F°
T(0)	= Temperature of fluid at bottom of fuel element, F°
T(L)	= Temperature of fluid at top of fuel element, F°
V	= Fluid velocity, ft/hr
P	= Pressure, lb/ft^2

FIG. IV - 3

THERMAL SELF-SHIELDING FACTOR VS WEIGHT % NATURAL BORON

FRESH CORE WITH CONTROL RODS AT 68°F (SPECTRAL HARDENED)

POISON ELEMENTS:
THICKNESS - 1/16"
EFFECTIVE LENGTH - 30"
WIDTH - 10.2" (SINE WAVE FORM)

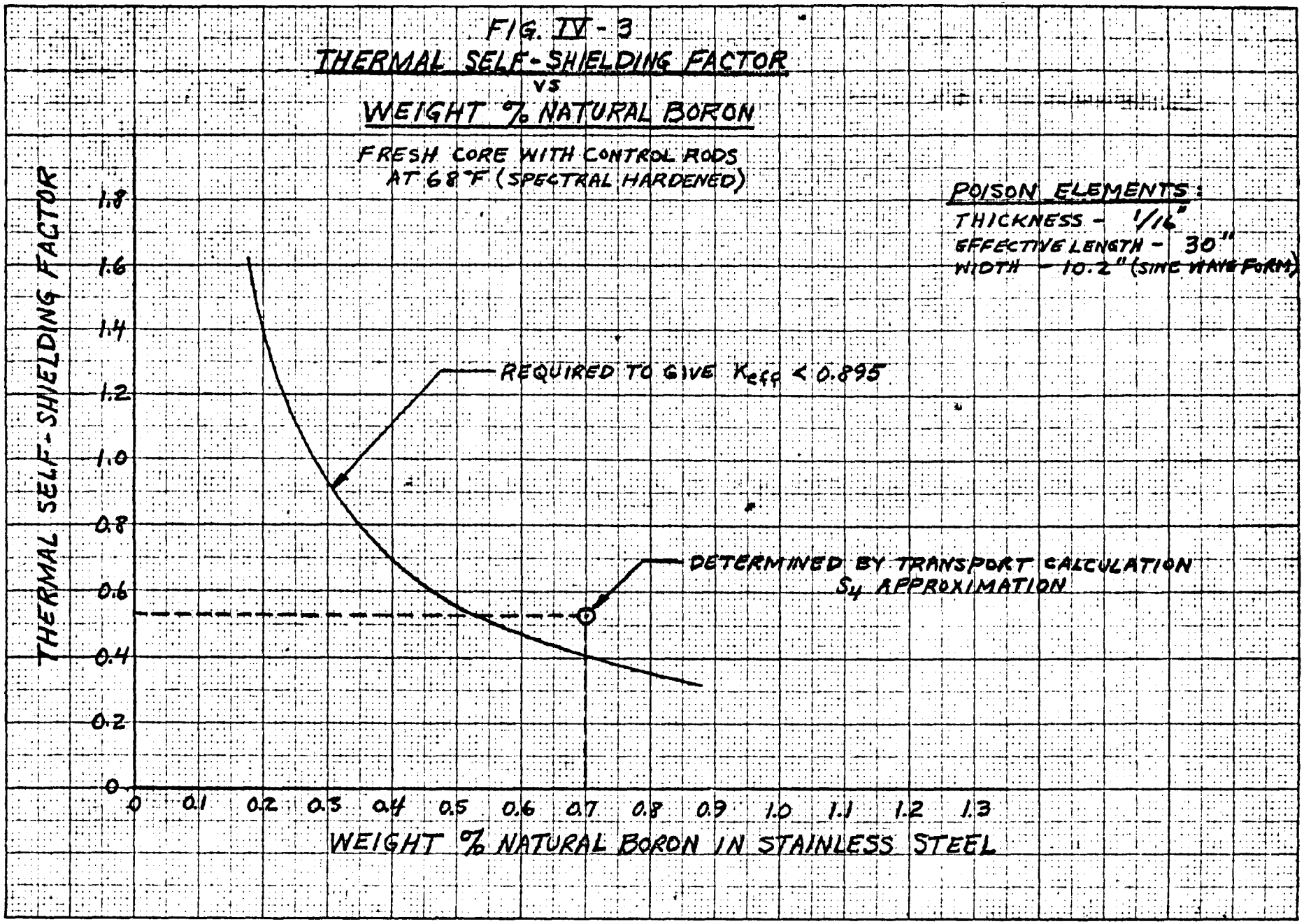

TABLE V - 1 (Continued)

ρ	= Density, lb/ft^3
F	= Friction head
β	= Density-temperature coefficient
$\bar{T}_i$	= Average fluid temperature inside element
$\bar{T}_o$	= Average fluid temperature outside element
A	= Flow area, ft^2
P_o^H	= Heat transfer perimeter of lead cask on inside surface, ft
f	= Friction factor
D	= Equivalent diameter, ft
h_o	= Heat transfer coefficient at cask wall, $BTU/(ft^2)(hr)(F°)$
k	= Thermal conductivity of liquid, $BTU/(hr)(ft)(F°)$
c_p	= Specific heat of liquid

2. Calculations - Laminar flow conditions exist in the cask so that

$$f = \frac{16}{\left(\frac{\rho V D}{\mu}\right)}$$

and

$$h_o = 1.75 \frac{k}{D_o} \left(\frac{\rho V_o A_o C \beta}{kL}\right)^{1/3}$$

Using these relations, equation (14) can be solved for $A_i V_i$, or

$$(A_i V_i)^{2.67} = C \frac{Q P_o^H}{D_o} \frac{1}{\left(\frac{1}{A_i D_i^2} + \frac{1}{A_o D_o^2}\right)}$$

$$C = \frac{7\beta g}{1536 \mu C_p} \left(\frac{Lk}{C_p \rho}\right)^{2/3}$$

For the core,

$$A_i = 217 \text{ in}^2$$

$$P_i = 3540 \text{ in}$$

$$D_i = \frac{4A}{P} = .245 \text{ in}$$

$$A_i D_i^2 = 13.05 \text{ in}^4$$

For the 3/8- in. annulus between the core and the inside perimeter of the cask wall,

$$A_o = 3/8\,\pi\,(23\text{-}13/16) = 27.2 \text{ in}^2$$

$$P_o = \pi\,(24 + 23\text{-}5/8) = 148.7 \text{ in}$$

$$D_o = \frac{4A}{P} = \frac{4(27.2)}{148.7} = .732 \text{ in}$$

$$P_o^H = \pi\,(24) = 75.4 \text{ in}$$

$$A_o D_o^2 = 14.55 \text{ in}^4$$

The coefficient C does not vary greatly with temperature so that it can be evaluated by assuming $T_{av} = 175°F$. Then,

$T_{av} = 175°F$ $\qquad$ $\bar{\rho} = 60.7$

$k = .389$ $\qquad$ $\beta = 3.64 \times 10^{-4}$

$c_p = 1.0017$ $\qquad$ $Q = 2KW = 6.83 \times 10^3 \frac{BTU}{hr}$

$\mu = .871$ $\qquad$ $L = 45$ in

Substituting these values, we get $C = 68.9$,

and

$$\frac{Qp_o^H}{D_o} = 7.05 \times 10^5$$

and

$$(A_i V_i)^{2.67} = (68.9)(7.05 \times 10^5)\frac{1}{\left(\frac{1}{18.05} + \frac{1}{14.55}\right)(12)^4}$$

$$= 1.61 \times 10^4$$

Thus,

$$A_i V_i = A_o V_o = (1.61 \times 10^4) \frac{1}{2.67} = 36.3 \frac{ft^3}{hr}$$

and

$$V_i = 24.1 \frac{ft}{hr}, \quad V_o = 192 \frac{ft}{hr}$$

also,

$$N_{Re_i} = 34.3$$

$$N_{Re_o} = 816, \text{ so that the flow is laminar as was assumed.}$$

Knowing the velocities, α and γ can be evaluated and the fluid temperatures calculated. Thus,

$$h_o = 1.75 \frac{k}{D_e} \left(\frac{\rho V_o A_o}{kL} \right)^{1/3} = 128$$

$$\alpha = \frac{h_o p_o^H}{C_p \rho V_o A_o} = .364, \quad \alpha L = 1.37, \text{ and } \gamma = \frac{Q}{C_p \rho V_o A_o} = 3.10$$

The temperature at the top of the cask is

$$T(L) - T_o = \frac{\gamma}{1 - e^{-\alpha L}} = 4.15°F,$$

and at the bottom of the cask

$$T(0) - T_o = \frac{\gamma e^{-\alpha L}}{1 - e^{-\alpha L}} = 1.06°F.$$

B. Temperature Drop Through the Lead

The temperature drop through the lead wall of the cask can be conservatively approximated by the temperature drop through the wall of a section of length L cut out of an infinite hollow cylinder.

Thus,

$$\Delta T_{pb} = \frac{Q}{2\pi L k_{pb}} \ln \frac{R_2}{R_1}$$

where

$$Q = 6.38 \times 10^3 \frac{BTU}{hr}$$

$$k_{pb} = 19$$

$$R_1 = 12.25 \text{ in.}$$

$$R_2 = 20.25 \text{ in.}$$

$$L = 45 \text{ in.},$$

and $\Delta T_{pb} = 7.66°F.$

C. Heat Transfer From Outside of the Cask

Heat will be transferred from the outside of the cask to the surrounding air by convection and radiation. Vertical fins have been placed around the outside perimeter of the cask to increase the heat transfer area. Heat loss by radiation from the outside has been neglected to provide an additional safety factor.

1. Development of Heat Transfer Equation - As in the treatment of natural circulation in the cask, the Bernoulli equation is integrated around the fluid flow path (up through the fins and into the ambient air). Neglecting VdP, we have:

$$T(Z) = (T_a - T_o)e^{-\alpha Z} + T_o$$

$$\alpha = \frac{h_{eff} P}{C_p \rho V A}$$

$$-\oint \rho \, dZ = L(\rho_a - \bar{\rho})$$

$$\bar{\rho} = \frac{1}{L} \int_o^L \frac{p}{RT} \, dZ$$

$$\rho_a - \bar{\rho} = \frac{P}{R}\left\{\frac{1}{T_a} - \frac{1}{T_o} - \frac{1}{\alpha L T_o} \ln\left[\frac{T_o + (T_a - T_o)e^{-\alpha L}}{T_a}\right]\right\}$$

$$= \rho_a \left\{1 - X - \frac{X}{\alpha L} \ln\left[\frac{1}{X} + \left(1 - \frac{1}{X}\right)e^{-\alpha L}\right]\right\}$$

$$T_o - T_a = \frac{Q}{VAC_p\rho_a(1 - e^{-\alpha L})}$$

$$\frac{1}{X} = 1 + \frac{Q}{VAC_pT_a\rho_a(1 - e^{-\alpha L})} = \frac{T_o}{T_a}$$

Equating the buoyant pressure to the friction pressure drop yields

$$L\rho_a \left\{1 - X - \frac{X}{\alpha L} \ln\left[\frac{1}{X} + \left(1 - \frac{1}{X}\right)e^{-\alpha L}\right]\right\}$$

$$= 4f\left(\frac{L}{D}\right)\rho\left(\frac{V^2}{2g}\right) + 1.4\,\frac{V^2}{2g}$$

where

T_a = absolute ambient temperature

T_c = cask wall temperature

$h_{eff} = h\eta$ (Ref. V-1, p. 236)

A = flow area between fins around entire cask perimeter

P = total heat transfer perimeter around fins and cask surface

The addition of 1.4 velocity heads to the pressure drop compensates for entrance and exit losses.

2. Calculations - The fins are 3 inches long, 3/16-inch thick, 4.5 feet high, and spaced on 1-3/16 inch centers around the outside of the cask. The fin efficiency is

$$\eta = \frac{\tanh\sqrt{2b}}{\sqrt{2b}}, \text{ where } b = \frac{hl^2}{kt}$$

where

l = fin length = 3 inches

h = heat transfer coefficient

k = thermal conductivity of fin = 9 Btu/(hr)(ft)(F°)
(stainless steel)

t = fin thickness (3/16 inch)

The temperature of the cask is determined by guessing a value of $\frac{Q}{\rho_a VACp}$ and calculating the cask temperature. Then a check is made to assure that the buoyant pressure is equal to or greater than the pressure drop.

Assume $\frac{Q}{\rho_a VACp} = 33°F$

$Q = 6.83 \times 10^3$

Number of fins = 109

$P = \frac{109 \times 7}{12} = 62.5$ ft

$A = \frac{3 \times 1 \times 109}{144} = 2.27$ ft^2

$T_a = 590°R$

Cp = .24 BTU/lb °F

k = .017 BTU/hr ft °F

V = .048 lb/ft hr

$\rho = .063$ lb/ft^3

$D_E = \frac{4 \times 2.27}{62.5} = .145$ ft

$\rho_a VACp = 207$

$\rho V = 380$

$$h_o = 1.75 \frac{k}{D_E} \left(\frac{\rho V_o A_o}{kL}\right)^{1/3} = 1.75 \frac{.017}{.145} \left(\frac{207}{.24 \times 109 \times .017 \times 4.5}\right)$$

$$= .965$$

$$b = \frac{.965 \times 9}{9 \times 3/16 \times 12} = .428$$

$$\sqrt{2b} = .930$$

$$\eta = \frac{\tanh \sqrt{2b}}{\sqrt{2b}} = \frac{.737}{.930} = .787$$

$$h_{eff} = \Sigma \eta h = .785$$

$$\alpha = \frac{.785 \times 62.5}{207} = .237$$

$$e^{-\alpha L} = e^{-1.07} = .344$$

$$(1 - e^{-\alpha L}) = .656$$

$$\frac{1}{X} = \frac{T_o}{T_a} = 1 - \frac{6.83 \times 10^3}{207 \times 590 \times .656} = 1.0853$$

$$(T_o - T_a) = 50°F$$

Buoyant pressure is given by

$$P_B = 4.5 \times .063 \left[1 - .921 - \frac{.921}{1.07} \ln \left[1.0853 - (1 - 1.0853).344\right]\right]$$

$$= .0088 \ .$$

Actually, the buoyant pressure is somewhat higher because the air jets at the top of the cask extend the effective length.

Friction and turning losses are given by

$$\Delta P_{f+t} = \frac{380 \times 6040}{2 \times 4.18 \times 10^8} \left[\frac{64}{1150} \times \frac{4.5}{.145} + 1.4\right] = .0086$$

Since the available pressure is greater than the pressure drop, the temperature drop is satisfactory. The Reynolds number of 1150 is in agreement with the assumption of laminar flow.

Even with this conservative calculation, the total temperature difference between the ambient air temperature and the maximum water temperature is 4.2° + 7.7° + 50° 62°F. Thus, the water will be under 192°F with the 125°F ambient assumed. Sizeable contributions to the heat transfer may also be expected from end losses and radiation losses.

At an altitude of 30,000 feet, the boiling point of water is lowered to 157°F. However, the ambient temperature in the plane is no higher than 70°F so that the temperature difference between boiling point and ambient at 30,000 feet is approximately the same as that for the assumed ground conditions. Pressure transients will not exist as the aircraft rises to 30,000 feet since the temperatures at the reactor plant sites are considerably less than the 125°F ambient assumed for the design.

The profile of the cask makes the actual fin area slightly greater than that used in these calculations. However, this has been neglected to simplify the calculations.

VI HEAT TRANSFER - "DRY" CASK

This chapter presents the heat transfer analysis of the shipping cask loaded with a spent core under loss of coolant conditions. Coolant loss from the cask may occur during its shipment to the reprocessing facility. The "dry" core is analyzed to determine the consequent maximum fuel element temperature due to fission product decay heat. This peak temperature is then compared to the allowable fuel temperature based on fuel element rupture discussed in Chapter VII.

A. Heat Transfer Analysis

The heat transfer analysis is based on the continuous generation of 2 KW of spent core after-heat. This heat rate corresponds to two years of full power operation and a subsequent one year storage at the reactor plant.

The "dry" core is cooled by means of air circulation between hot fuel elements contained within the core shroud and the inside cask wall. Air flow is maintained, in steady state conditions, by means of a static head difference between air located within the core and that column of air in an annulus at the inside perimet r of the cask wall. This pressure difference is based on uniform axial power generation in the core and a constant cask wall temperature. A constant wall temperature is assumed because of the relatively high conductivity of the combination stainless steel - lead cask wall. The calculated temperature profiles indicate that the core acts as a hot leg and the annulus as a cold leg. Thus, air flows in a loop up through the fuel elements and down between the core shroud and the inside perimeter of the cask (see Fig VI-1).

FIG. VI - 1

COOLANT FLOW PATH IN SHIPPING CASK

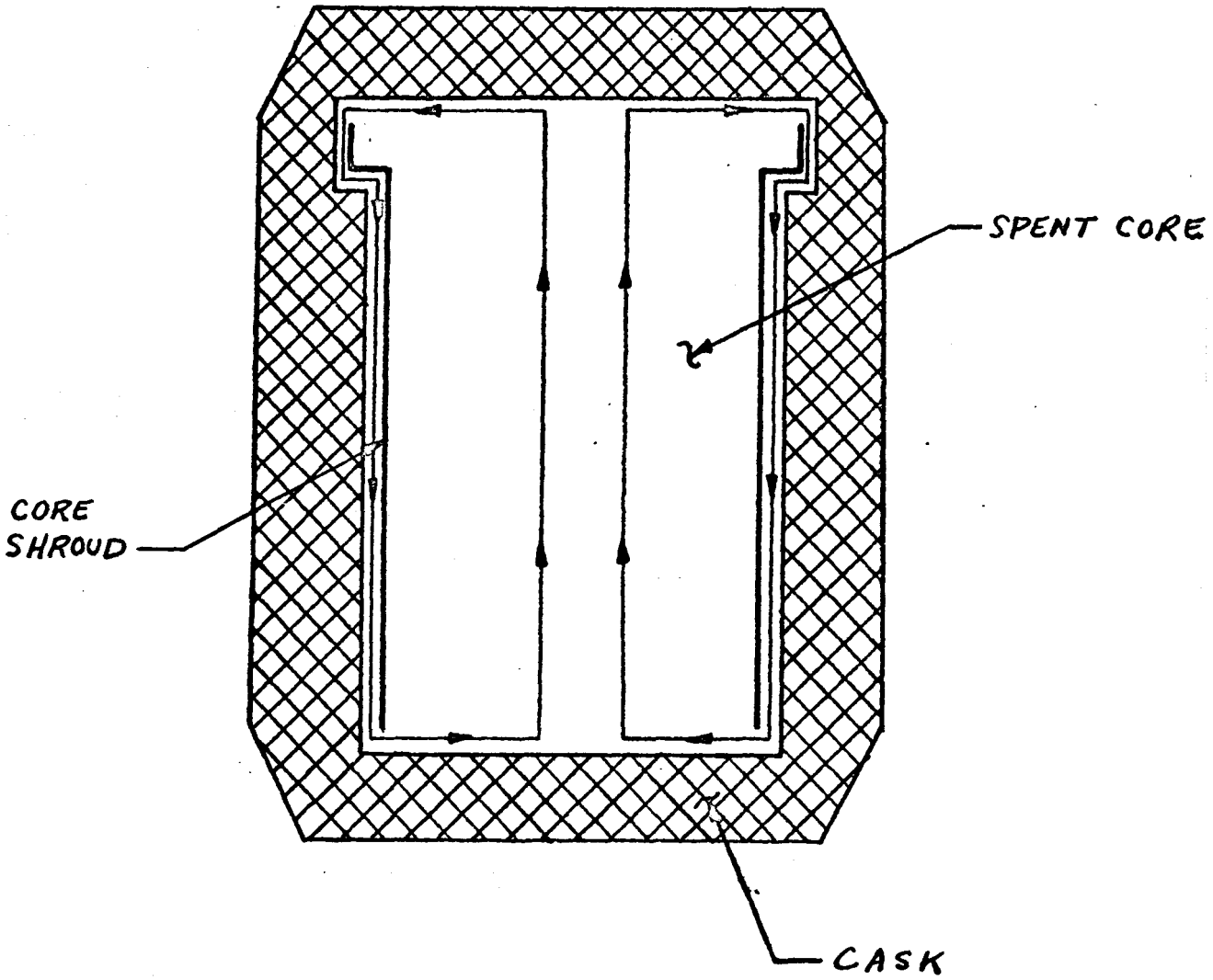

Additional assumptions were made to simplify the analytical calculations; namely, cross flow of air in the core was neglected, and in regions above and below the core perfect mixing of air was assumed.

A conservative analysis is established by neglecting the heat transfer benefits of:

1. Radiation from the core to the cask wall, and
2. Heat transfer from the top and bottom of the cask.

To determine the maximum fuel element temperature, trial and error calculations were performed. Heat transfer coefficients, friction flow losses and static pressures are calculated. The air outlet temperature for an average fuel element and the hottest element are computed as well as temperature changes across the element and fuel matrix. These temperature changes are added to the air outlet temperature, resulting in a maximum fuel matrix temperature.

1. Development of Heat Transfer Equations - The equations used to determine the inside cask wall temperature are identical to those presented in Chapter V.

The relationships employed for heat transfer within the cask are the conventional convection and conduction equations. The heat transfer coefficient, h^*, is calculated as follows (Ref. VI-1):

$$h = 1.5 \frac{k_b}{D_e} \left[\frac{m_t C_{pb}}{k_b L} \right]^{.4} \qquad (1)$$

where $$m_t = 3600 \, V \, a \, \rho_m \qquad (2)$$

Since the heat flux across the cask wall is constant for a specified

---

* See Table VI-1 for nomenclature.

after-heat duty, the log mean temperature change in the annulus is a function of the heat transfer coefficient,

$$MTD = \left(\frac{q}{A}\right) / h \tag{3}$$

The air temperature change is found by the following relation

$$\Delta t = q/(m_t\ C_{pb}) \tag{4}$$

Values derived from Eq 3 and Eq 4 are substituted into the following relation defining log mean temperature difference:

$$MTD = \frac{(t_o - t_w) - (t_i - t_w)}{\ln \frac{t_o - t_w}{t_i - t_w}} \tag{5}$$

The relation,

$$t_o = t_i + \Delta t \tag{6}$$

is substituted into Eq 5 and the explicit solution for the coolant temperature leaving the annulus is

$$t_i = \frac{t_w - \Delta t - (t_w\ e^{\Delta t/MTD})}{1 - e^{\Delta t/MTD}} \tag{7}$$

Coolant temperature at the top of the annulus is readily found from Eq (6). The average coolant temperature is calculated by

$$t_{avg} = \frac{t_i + t_o}{2} \tag{8}$$

The calculated temperatures are used to determine the static pressure in the core and the annulus. In the core, the

static head is

$$\Delta P_c = \rho_i Z_i + \rho_m Z_e + \rho_o Z_o \qquad (9)$$

where (Ref. VI-2)

$$\rho = p/(346.5 + .7535\ t) \qquad (10)$$

and

$$\rho_m = p/(346.5 + .7535\ t_{avg.}) \qquad (11)$$

The annulus static head is found as follows. The temperature profile is calculated according to (see p. V-2, eq.7):

$$t(Z) = \left[t(L) - t_w \right] e^{-\alpha (L-Z)} + t_w \qquad (12)$$

Equation 12 is derived in Chapter V and its application in this section neglects any effects of compressibility. The shape of the temperature profile is determined by the α term where

$$\alpha = h\ P_w^H / (C_{pb}\ m_t) \qquad (13)$$

Temperatures are calculated along the cask wall. Each computed value is substituted into Eq (10) to determine the coolant density. The density profile is then integrated by Simpson's method.

$$\Delta P_a = \sum_{i=0}^{i=n} \frac{d}{3} \left[\rho_i + {}^4\rho_{i+1} + {}^2\rho_{i+2} + {}^4\rho_{i+3} + \cdots \rho_n \right] \qquad (1$$

The difference between the static pressure in the annulus and the core is balanced by the frictional flow losses of the loop. Laminar flow exists in the coolant circuit, and the pressure loss due to skin friction in the core is

$$\Delta P_c = \frac{32 \mu_m L V_c}{3600\ g_c\ D_e^2} \qquad (15)$$

The associated skin friction loss in the annulus is found for compressible fluid flow by integrating the following equation:

$$-\frac{dP_f}{dZ} = \frac{12\,\mu\,G}{z^2\,g_c\,\rho} \tag{16}$$

Correcting Eq. 16 for units, the pressure drop is

$$-\int_o^L dp = \Delta P_a = \frac{12\,G}{(3600)^2\,z^2 g_c}\int_o^L \frac{\mu(z)}{\rho(z)}\,dZ \tag{17}$$

$$\Delta P_a = C\int_o^L \frac{\mu(z)}{\rho(z)}\,dZ \tag{18}$$

Simpson's method, Eq. 14, is again used to evaluate the integral.

Additional pressure losses are calculated for expansion and contractions of the coolant in the loop and for changes in flow direction. These losses are found by

$$\Delta P_r = K_r\,\frac{V^2}{2g_c}\,\rho \tag{1 }$$

where K_r is the sum of the constants used to compute the individual velocity head losses around the loop. Therefore, the steady state velocity through the annulus (or the core) is found by the following expression:

$$\int_o^Z \rho(z)\,dZ - \left[\rho_i\,Z_b + \rho_m Z_e + \rho_o Z_h\right] = \Delta P_c + \Delta P_a + \Delta P_r \tag{20}$$

(annulus) (core) (loop)

Equation (20) balances the net static head available between the core and annulus with the total frictional pressure drop of the coolant loop.

To determine the air outlet temperature from the hottest fuel element the total pressure drop of an average core element is equated to the pressure drop of the hot element. Based on previous analyses performed on the PM-1 core, a radial power factor of 1.5 is assumed. The power factor for a spent core is approximately the same as for a fresh core. As a result of additional detailed heat transfer analyses performed on the PM-1 core, it is known that the heat transfer split between the inside and outside of the fuel element tubes is very nearly equal. The "dry" core will behave in an essentially identical manner. Assuming various outlet temperatures the pressure drop available for frictional losses is found from the relation,

$$(\Delta P_{st} + \Delta P_f)_{avg} = (\Delta P_{st} + \Delta P_f)_{hot} \qquad (21)$$

The left side of Eq (21) is a known constant. The outlet temperature determines the hot element static head. Equation (21) is solved for the hot element friction loss; the coolant velocity is found by Eq 15. The mass flow rate is computed by Eq (2). A heat balance, Eq (4), is made across the hot element to determine coolant flow rate as a function of outlet temperature. The heat balance and flow equations are solved for outlet temperature and coolant velocity. Eq (1) is then used to calculate the hot element heat transfer coefficient which is substituted into Eq (3) to determine the MTD. It is assumed that the film temperature change is constant axially along the element. Thus, the maximum clad temperature equals the air outlet temperature plus the MTD.

The temperature rise across the clad is

$$\Delta t = q \chi / k A \qquad (22)$$

In this equation, the power term accounts for the heat split between the inside and outside walls of the hot element and the radial power factor.

The matrix fuel temperature rise for the tubular elements is calculated from the following equation (Ref VI-3):

$$t_{max} - t_1 = \frac{H_1 r_1^2 (1 - \beta + \beta \ln \beta)}{4 k_1} \qquad (23)$$

Application of Eq (23) assumes that the inside and outside clad temperatures are equal. The fuel matrix (75% stainless steel, 25% uranium oxide) thermal conductivity is estimated to be 75% of the conductivity of stainless steel.

TABLE VI-1 NOMENCLATURE FOR HEAT TRANSFER ANALYSIS - "DRY" CASK

a	- Cross sectional flow area, ft^2
A	- Surface area of heat transfer, ft^2
C_p	- Specific heat of air, Btu/lb °F
d	- Incremental distance Eq (14), ft
D_e	- Equivalent diameter, ft
f	- Friction factor
g_c	- Conversion factor, 32.2 lb_m-ft/(lb_f)(sec^2)
h	- Surface coefficient of heat transfer, Btu/(hr)(ft^2)(°F)
H	- Volumetric rate of heat production in fuel element, Btu/(hr)(ft^3)
K	- Number of velocity heads
k	- Thermal conductivity, Btu/(hr)(ft)(°F)

L - Length, ft

m - Air mass flow rate, lb/hr

MTD - Log mean temperature difference, deg. F

n - Total number of fuel elements, 741

p - Atmospheric pressure, 29.92 in Hg.

P - Pressure, psf

P_o^H - Heat transfer perimeter of load cask on inside surface, ft

q - Average power, Btu/hr

r - Inside radius of fuel element, ft

S - Cross sectional area of flow, sq ft

t - Temperature, °F

V - Average linear velocity, ft/sec

χ - Fuel element clad thickness, ft

z - Clearance between core shroud and inside of cask wall, ft

Z - Vertical height, ft

α - Ratio in Eq (13), ft^{-1}

β - Dimensionless ratio

Δt - Temperature potential, °F

μ - Viscosity of air, lb/hr ft

ρ - Density of air, lb/ft^3

Subscripts

a - Annulus

avg - Average

b - Bulk

c - Core

f - Skin friction loss Eq (16)

h - Height above core

hot - Hottest fuel element Eq (21)

i - Inlet of core

m	- Mean
max	- Maximum
o	- Outlet of core
r	- Flow losses, other than skin friction
st	- Static pressure, Eq 21
t	- Total
w	- Wall
1,2	- Inside and outside of fuel element surfaces respectively

---

2. Calculations - The first step in the calculations is to assume a bulk temperature and pressure to evaluate the coolant physical properties. In this analysis, the coolant pressure is atmospheric. Let the initial average temperature be 400°F. The air bulk properties are thus

$$C_p = 0.250 \text{ Btu/lb °F}$$

$$k = 0.0225 \text{ Btu/lb °F ft}$$

$$\rho_m = 0.0462 \text{ lb/ft}^3$$

Equation (2) yields the mass flow rate assuming a 1.65 ft/sec average velocity in the annulus.

$$\dot{m}_t = 3600\, a \rho_m V_a \qquad (2)$$

The cross sectional flow area of the annulus, a, is 0.229 ft^2.

$$\dot{m}_t = (3600)(0.229)(0.0462)\ (1.65)$$

$$\dot{m}_t = 62.9 \text{ lb/hr}$$

The heat transfer coefficient at the inside wall is calculated.

$$h = 1.5 \frac{k_b}{D_e} \left(\frac{\dot{m}_t C_{pb}}{k_b L} \right)^{.4} \qquad (1)$$

where $D_e = .0726$ ft

$L = 4.12$ ft

$$h = 1.5 \frac{0.225}{.0726} \left(\frac{62.9 \times 0.250}{0.0225 \times 4.12} \right)^{.4}$$

$$h = 3.63 \text{ Btu/hr ft}^2 \text{ °F}$$

The log mean temperature difference is

$$MTD = \frac{q}{A\,h} \qquad (3)$$

where $q = 6826$ Btu/hr

$A = 26.82$ ft^2

$$MTD = \frac{6826}{(26.82)(3.63)}$$

$$MTD = 70.1 \text{ °F}$$

The average air temperature change is then calculated,

$$\Delta t = q/(m_t c_{pb}) = \frac{6826}{(62.9)(0.250)} \qquad (4)$$

$$\Delta t = 434 \text{ °F}$$

The inlet air temperature to the core is found

$$t_i = \frac{t_w - \Delta t - \left(t_w e^{\frac{\Delta t}{MTD}} \right)}{1 - e^{\Delta t/MTD}} \qquad (7)$$

where $t_w = 183$ °F

$$t_i = \frac{183 - 434 - \left(183\, e^{\frac{434}{54.9}}\right)}{1 - e^{434/54.9}}$$

$$t_i = 184.5 \text{ °F}$$

The air outlet temperature, from Eq (6), is

$$t_o = t_i + \Delta t$$

$$= 184.5 + 434 = 618.5 \text{ °F}$$

The average coolant temperature

$$t_{avg} = \frac{t_i + t_o}{2} \qquad (8)$$

$$= (184 + 618.5)/2$$

$$= 401.5\ ^\circ F$$

Recalling that the assumed t_{avg} was 400 °F, no new bulk temperature is assumed.

The static head in the core segment of the loop is

$$\Delta P_c = \rho_i Z_i + \rho_m Z_c + \rho_o Z_o$$

where $Z_i = 0.75$

$Z_c = 2.5$

$Z_o = 0.96$

$$\rho_o = P/(346.5 + .7535\ t_o) \qquad (10)$$

$$\rho_o = 0.0369\ lb/ft^3$$

Similarly $\rho_i = 0.0616\ lb/ft^3$

and $\rho_m = 0.0462\ lb/ft^3$

$$\Delta P_c = (0.0616)\ (.75) + (0.0462)\ (2.5) + (0.0369)\ (0.96)$$

$$= 0.1971\ psf$$

The annulus temperature profile is evaluated from Eq (12)

$$t(Z) = \left[t(L) - t_w\right] e^{-\alpha (L-Z)} + t_w$$

where $L = 4.12$ ft

$t_w = 183°F$

$P_w^H = 6.32$ ft

and

$$\alpha = \frac{h\ P_w^H}{C_{pb}\ m_t} \qquad (13)$$

$$\alpha = \frac{(3.63)\ (6.32)}{(.250)\ (62.9)} = 1.459$$

To determine point temperature values, axial increments of 0.4 feet are used. At each point along the wall, air density is computed (Eq 10). The total static head in the annulus is determined by Simpson's method of integration. The results of the integration are shown in Fig VI-2. For this case, the static head is 0.2325 psf. The net static head is 0.2325 - 0.1971 = 0.0354 psf.

The frictional flow pressure drops are next calculated. The core pressure drop by Eq (15)is:

$$\Delta P_c = \frac{32 \mu_m L V_c}{3600\ g_c D_e^2}$$

where $\mu_m = 0.063$ lb/ft hr

$= 1.75 \times 10^{-5}$ lb/ft sec

$D_e^* = 0.0347$ ft

$L = 2.5$ ft

The average velocity of coolant in the core, V_c, is calculated as follows:

$$V_c = V_a \frac{S_a}{S_c}$$

where

$S_a = 0.229$ sq ft

$S_c = 2.33$ sq ft

$$V_c = (1.65) \frac{(0.229)}{(2.33)} = 0.1625 \text{ FPS}$$

The Reyonlds' number is checked for laminar flow conditions

$$R_e = \frac{D_e V \rho_m}{\mu_m}$$

---

* The hydraulic diameter equal to the inside diameter of the fuel element is used. The equivalent diameter of the outer section of an element is 5 per cent greater.

FIG. VI-2
COOLANT DENSITY PROFILE ALONG INSIDE WALL OF SPENT FUEL CASK

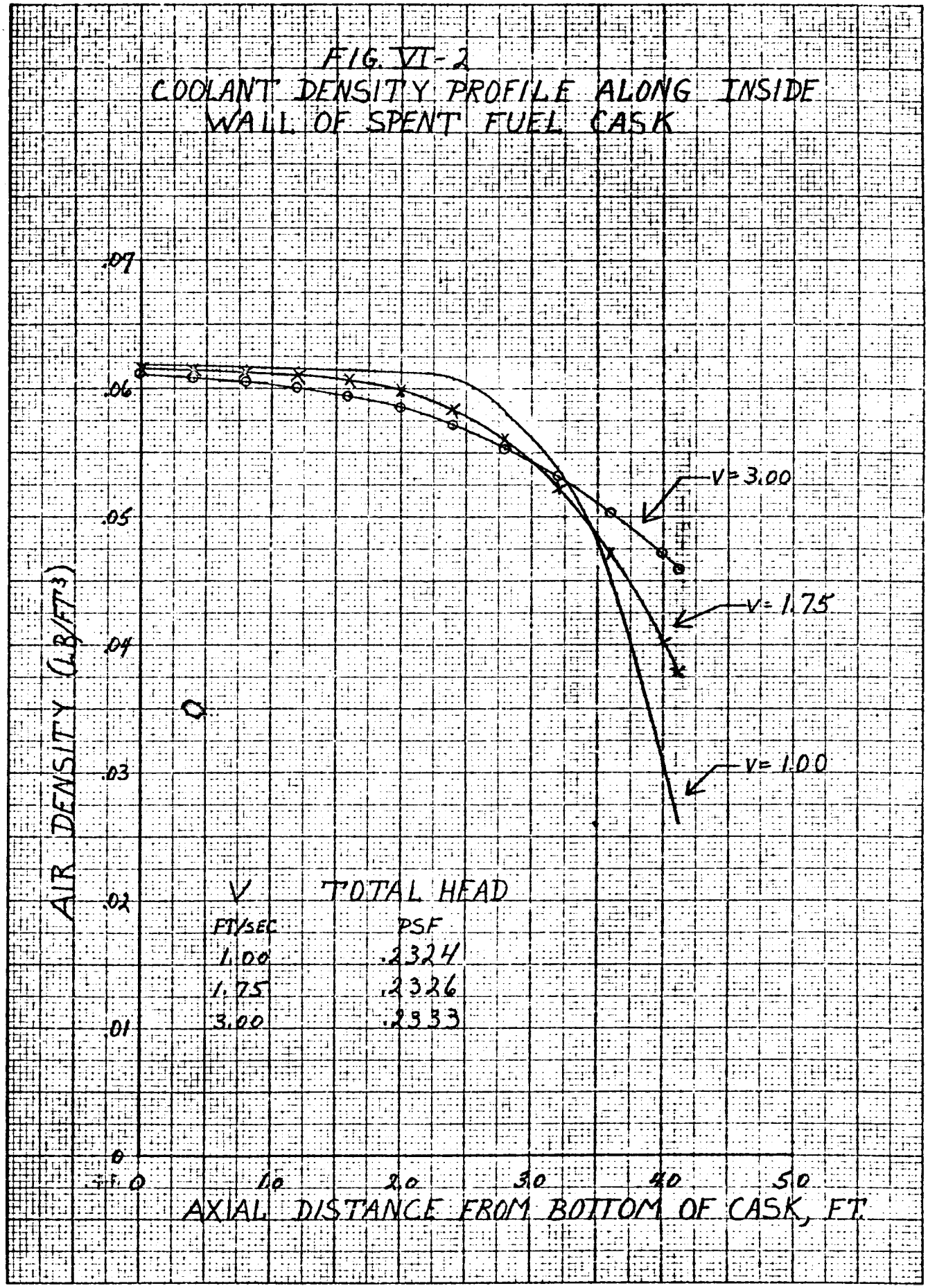

V FT/SEC	TOTAL HEAD PSF
1.00	.2324
1.75	.2326
3.00	.2333

$$= \frac{(0.0347)(0.1625)(0.0462)}{1.75 \times 10^{-5}} = 14.9$$

The Reynolds number is less than 2100; thus, laminar flow exists in the core. The pressure drop in the core is:

$$\Delta P_c = \frac{(32)(0.063)(2.5)(0.1625)}{(3600)\ (32.2)\ (0.0347)^2} = 0.00587 \text{ psf}$$

The pressure drop in the annulus is found from Eq 18 for annular velocities of 1.0, 1.75, 2.0 and 3.0 fps. At 1.75 fps calculation details are shown in Table VI-2

TABLE VI-2 COOLANT PRESSURE DROP IN ANNULUS

Z ft	t_{avg} °F	μ_m lb/ft hr	ρ_m lb/ft^3	μ_m/ρ_m ft^2/hr	Simpson's Sum
0.0	184.3	0.0510	0.0616	0.828	0.8280
0.4	185.4	0.0510	0.0615	0.829	3.3160
0.8	187.1	0.0511	0.0613	0.834	1.6680
1.2	190.2	0.0514	0.0611	0.840	3.3600
1.6	195.5	0.0516	0.0606	0.851	1.7020
2.0	204.7	0.0522	0.0598	0.872	3.4880
2.4	220.8	0.0531	0.0584	0.910	1.8200
2.8	248.8	0.0547	0.0561	0.975	3.9000
3.2	297.8	0.0574	0.0522	1.100	2.2000
3.6	382.0	0.0620	0.0472	1.312	5.2480
4.0	529.4	0.0693	0.0402	1.725	1.7250
					29.2550
d/3 = 0.4/3 = 0.1333					
				$\sum$ = 29.255 x 0.1333 =	3.8997
For the last increment,					
Z_{avg} = 4.06		0.0708	0.0390	1.815	
d = 0.120			$\sum$ = 1.815 x 0.120 =		.2178

$$\therefore \int_0^{L=4.12} [\mu(z)/\rho(z)]\, dz = 4.1175$$

Constant, $C = \frac{12\,G}{(3600)^2 \times 32.2}$

where $G = 297.4$ lb/hr ft^2

$\epsilon = 0.0364$ ft

$C = 6.45 \times 10^{-3}$

$\Delta Pa = 6.45 \times 10^{-3} \times 4.1175 = 0.0265$ psf

The annular pressure drop at 1.65 fps is 0.0235 psf.

Verification of laminar flow in annulus

$$Re = \frac{D_e V_a \rho_m}{\mu}$$

$\rho = 0.0616$ lb/ft^3

$V_a = 1.65$ fps

$D_e = 0.0726$ ft

$= 1.42 \times 10^{-5}$ lb/sec ft

$$Re = \frac{(0.0726)(1.65)(0.0616)}{1.42 \times 10^{-5}}$$

$Re = 521$

Therefore, laminar flow exists in the annulus.

Expansion and contraction pressure losses around the loop were based on K values versus inlet to outlet area ratios at a Reynold's number of 2000 (Ref. VI-4). A Reynold's number of 2000 was assumed for conservatism. A series of detailed calculations determined the effective areas of flow. Coolant densities were taken at four points along the annulus; namely, (a) at the cask top (Z = 4.12 ft), (b) 0.75 ft below the top (Z = 3.4 ft), (c) 1/2 the distance from the cask bottom to the core "ledge" (Z = 1.7 ft), and (d) at the cask bottom (Z = 0). These densities were used to account for the large variation in coolant density along the annulus. At several places in

the annulus 90° changes in flow direction occur. The pressure losses for these right angle turns are approximated to be 0.1 of a velocity head. To simplify calculations, these small velocity head losses and the expansions and contractions in the core are neglected. Results are tabulated in Table VI-3 at V_a = 1.65 fps.

TABLE VI-3 EXPANSION AND CONTRACTION PRESSURE LOSSES

Z	K	K*	ρ (lb/ft^3)	ΔP psf
4.12	0.860	1.375×10^{-2}	0.0368	0.00138
3.4	0.830	1.870×10^{-2}	0.0581	0.00295
1.7	0.400	6.220×10^{-3}	0.0607	0.00130
0	0.520	8.400×10^{-4}	0.0616	0.00014
				0.00550 psf (total)

The core, annulus, and expansion frictional losses are added. The total pressure drop is 0.0349 psf which is less than the net static head of 0.0354 psf. Therefore, the steady state flow velocity will be slightly greater than 1.65 fps. Fig. VI-3 shows the total frictional pressure losses and net static head as a function of coolant velocity in the annulus. The intersection of these two curves graphically balances Eq (20). At steady state conditions, the design coolant velocity and average outlet temperature are 1.69 fps and 610°F, respectively.

The heat transfer calculations for the hot element are presented in the following paragraphs. The pressure drop of the

* Accounts for velocity ratio at different points based on annulus area and factor 1/2 g_o.

FIG. VI-3 FUEL CASK PRESSURE DROP CORRELATION

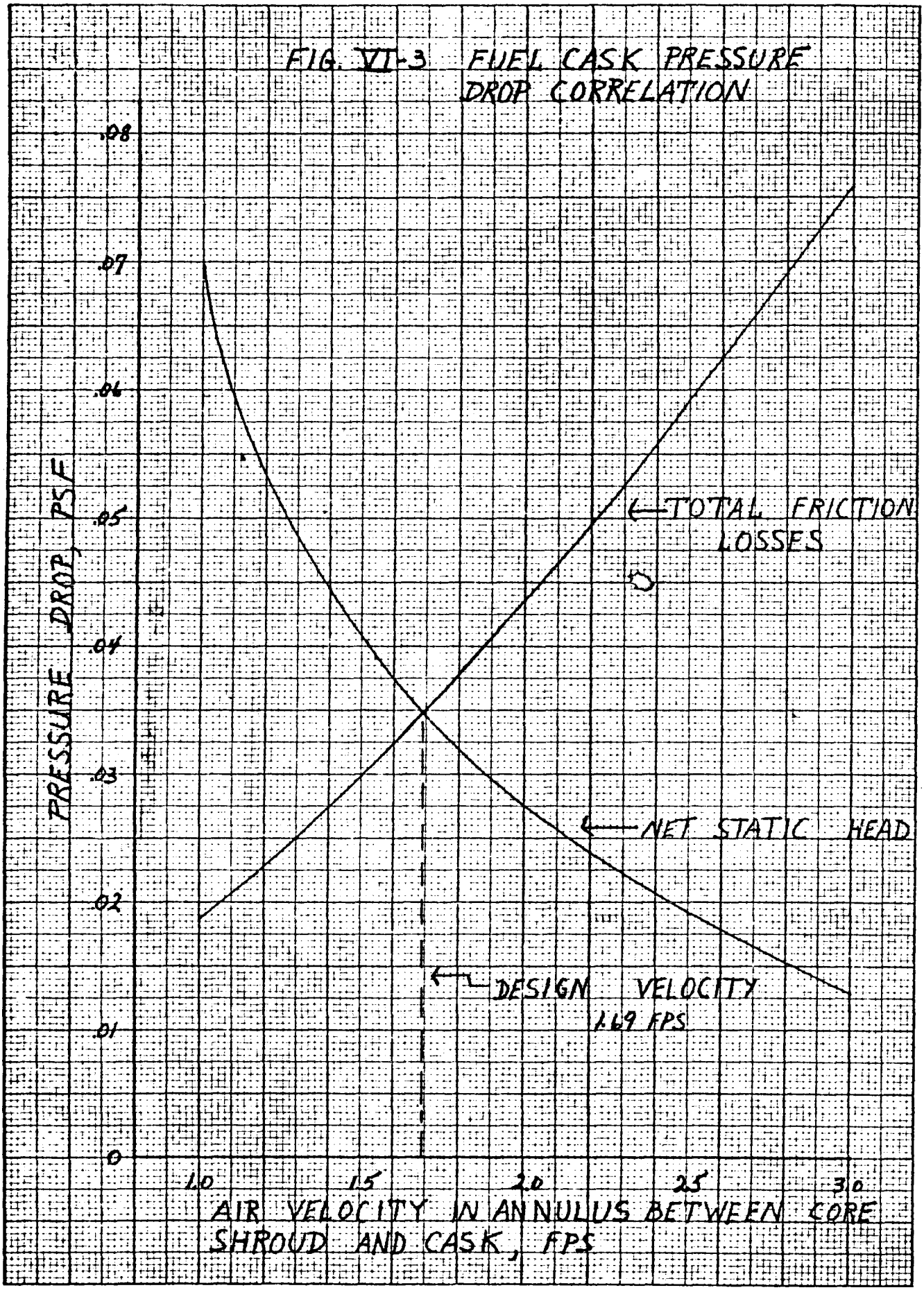

VI-15A

average element to be equated to the hot element pressure drop is found.

$$\Delta P = \frac{32 \mu_m L V_c}{3600 g_c D_e^2} + Z_e \rho_m$$

$$= \frac{(32)(0.0630)(2.5)(.01665)}{3600\ (32.1)\ (0.0347)^2} + (2.656)(0.0463)$$

$$= 0.1290 \text{ psf}$$

The straight length is increased from 2.5 ft to 2.656 ft to account for the small necked down portion of the fuel elements below the top grid plate. An outlet temperature of 716 °F is assumed. The hot element static head is

$$\Delta P_{st} = 2.656\ (0.0436)$$

$$= 0.1158 \text{ psf}$$

The net frictional head is

$$\Delta P_f = 0.1290 - 0.1158 = 0.0132 \text{ psf}$$

Coolant physical properties are evaluated at a mean temperature of 450°F. The velocity inside the hot element by Eq (15) is

$$V_c = \frac{(32.2)(0.0347)^2\ (3600)\ (0.0132)}{32\ (0.0656)\ (2.5)}$$

$$V_c = 0.351 \text{ ft/sec}$$

The mass velocity is

$$m = 3600\ a \rho V \qquad (2)$$

The cross sectional area of flow is the inside element flow area multiplied by the total number of fuel elements

$$a = (0.000945)\ (741) = 0.700 \text{ ft}^2$$

$$m = (3600)\ (0.700)\ (0.0436)\ (0.351)$$

$$= 38.6 \text{ lb/hr}$$

The heat balance is

$$\dot{m} = q_{hot} \quad / C_p (t_o - t_i)$$

$$q_{hot} = 6826 \times \frac{1.5}{2} = 5120 \text{ Btu/hr}$$

$$\dot{m} = \frac{5120}{(0.250)(716 - 184.5)}$$

$$\dot{m} = 38.5 \text{ lb/hr}$$

The mass flow rates are essentially balanced. The actual coolant outlet temperature is slightly less than 716°F.

The hot element heat transfer coefficient is

$$h = 1.5 \frac{k_b}{D_e} \left(\frac{\dot{m} C_p}{k_b L} \right)^{.4} \qquad (1)$$

where $k_b = 0.0290$ Btu/hr - ft - °F

$D_e = 0.0347$ ft

$C_p = 0.250$ Btu/lb °F

$L = 2.5$ ft

$\dot{m} = 38.5/741 = 0.519$ lb/hr

$$h = \frac{(1.5)(0.029)}{0.0347} \left[\frac{(0.519)(0.25)}{(0.029)(2.5)} \right]^{.4}$$

$h = 1.585$ Btu/hr ft^2 °F

The MTD along the hot element is

$$MTD = \frac{5120}{(1.585)(201.5)} = 16.0 \text{ °F}$$

The clad temperature at the top end of the hot element is thus 716 + 16 = 732 °F

The clad temperature change based on similar assumptions of heat split is:

$$\Delta t = \frac{q x}{k A} \qquad (22)$$

where $q = 5120$ Btu/hr

$\chi = 6.25 \times 10^{-4}$ ft

$k = 11.5$ Btu/hr ft °F

$A = 201.5$ ft ^{2}

$$\Delta t = \frac{(5120)(6.25 \times 10^{-4})}{(11.5)\ (201.5)}$$

$$= 1.38 \times 10^{-3} \text{ °F}$$

The clad temperature change is neglible.

The fuel matrix temperature rise is calculated from Eq (23).

$$t_{max} - t_i = H_1 r_1^2 \frac{(1 - \beta + \beta \ln \beta)}{4 k_1} \qquad (23)$$

where

$k_1 = 0.75\ k_{ss}$

$k_{ss} = 11.5$ Btu/hr ft °F

$k_1 = (0.75)\ (11.5) = 8.62$ Btu/hr ft °F

For the hot fuel element the volumetric rate of heat production is 18,450 Btu/hr ft^3. The values of the geometrical terms in Eq (23) are

$\beta = 0.525$

$r_1 = 0.01875$ ft

Therefore,

$$t_{max} - t_1 = \frac{(18{,}450)(0.01875)^2 \left[1 - (0.525) + (0.525)(-0.646)\right]}{(4)\qquad(8.62)}$$

$$= 0.026 \text{ °F}$$

The fuel matrix temperature rise is also neglible.

3. Results - The heat transfer calculations indicate the following characteristics for the average fuel element:

Inlet air temperature, °F	184.5
Outlet air temperature, °F	610
Average linear velocity, ft/sec	0.163
Power, Btu/hr	9.2

The convection loop pressure drop under steady state conditions is 0.0348 psf. Analysis of the hottest element with a 1.5 radial power factor increased the air outlet temperature to 716 °F and the average linear velocity to 0.35 ft/sec. The film temperature rise across the inside surface of the hottest tube is 16°F. The volumetric heat generation rate of the spent fuel matrix is small, resulting in a negligible temperature change within the tube wall and across the fuel clad.

The log mean temperature difference between the circulating air and the cask wall is calculated to be 70°F. The average air velocity through the annulus is 1.69 ft/sec resulting in a heat transfer coefficient at the wall of 3.63 Btu/hr ft^2 °F.

B. Conclusions

The maximum fuel temperature in the hottest element of a spent core contained within the spent fuel cask and cooled solely by air circulation is 732 °F. This is less than the predicted rupture temperature of 950°F for the stainless steel elements as given in Chapter VII. According to the AEC shipping regulation the allowable margin between the maximum fuel temperature and the rupture point is 200°F. The calculated temperature difference of 218°F is more than adequate to assure that the elements will not rupture under loss of coolant conditions. In addition, considerable conservatism is

included in the calculational methods by neglecting the heat transfer benefits derived from radiation effects and heat transfer to the top and bottom of the fuel cask. Conservatism is also provided by the assumption of a 125°F atmospheric temperature.

It is also concluded that no melting of the lead (melting point = 621°F) contained in the cask wall is possible based on the maximum wall temperature of 183°F. It was pessimistically assumed for this calculation that all of the core decay heat inpinges on the inside cask wall when in reality a portion of this heat is desposited in the lead shield directly.

On the basis of this analysis it is concluded that the spent core would not suffer damage due to temperature effects in the unlikely event of loss of coolant from the shipping cask.

VII. FUEL ELEMENT RUPTURE TEMPERATURE AND ACTIVITY RELEASE RATES

The proposed shipping regulations for spent fuel list two separate hazard areas that must be satisfied. The first concerns the maximum fuel temperature that can be allowed without causing damage to the individual fuel elements. The second assumes a specified accident condition and restricts the fission product release.

A. Fuel Element Rupture Temperature

The maximum allowable fuel element temperature at which no failure occurs must be based on one of the following criteria:

(1) The peak temperature of the elements during shipment must be no higher than the maximum temperature seen by the elements during operation for a minimum of 30 days.

(2) Fuel element temperature must remain 300°F below the average or 200°F below the lowest value for at least two (2) fuel elements evaluated experimentally. The failure criterion is: during 48 hours of immersed exposure the maximum amount of activity released must not exceed 100 curies of beta plus gamma or 0.1 curie of alpha activity.

(3) Fuel temperature must remain 200°F below that which would cause damage to structurally sound fuel.

As will be shown, the third criterion is used to establish the limiting temperature for the fuel elements by the conservative application of experimental test data.

1. Fuel Element Metallurgy Aspects - The fuel elements contain a 28.3 - 71.7% dispersion by weight of UO_2 and stainless steel powders clad with stainless steel. The dispersion contains fuel particles of approximately 50 - 100 microns in diameter and is nominally 0.0285 inch thick. The dispersion is sandwiched between inner and outer clads each of 0.0075 inch thickness.

Essentially each UO_2 particle or small group of particles is completely surrounded by stainless steel. Thus, each particle is contained within a small minute pressure vessel. This is most advantageous from the hazard standpoint since a fracture under an accident condition would expose only the UO_2 particles directly along the fracture plane. In addition, any subsequent corrosion would also be limited to just the exposed particles.

2. Discussion of Experimental Data - Due to the geometry and metallurgical aspects of the dispersion type fuel element, it becomes difficult to accurately calculate a limiting temperature by strictly analytical methods. Gaseous diffusion rates, pressure build up, and reasonable stress techniques do not lend themselves to an application of such a minute size. Various attempts have been made (ref. VII-1), but the parameters and assumptions are too widespread and variable to provide any confidence in the results.

Unfortunately, experimental results on irradiated PM-1 elements, or, in fact, UO_2 dispersion elements of any dimensions, are not available at the burn-up and temperatures of interest.

However, work performed at the Battelle Memorial Institute has produced correlations which can be applied to the PM-1 type fuel element.

The information presented in the Battelle report (ref. VII-2) proposes a creep-failure model and criteria are developed from the model which permits estimates of the relative severity of tests performed under different test conditions. Basically, the failure model is described, an analytical evaluation is made for the various parameters, and the unknown constants evaluated by an experimental program. In this manner, an extrapolation may be made to the burn-up and environmental conditions expected for the PM-1 type element.

The type of fuel elements tested by BMI, UO_2 dispersions in stainless steel, is similar to the PM-1 element except for geometry. However, with a conservative application of the BMI results, an acceptable comparison of the elements can be made since the significant parameters affecting the tests including weight percent of UO_2, fuel element temperature, etc., are in the range of the PM-1 elements. Therefore, since this information was found to be a reasonable correlation and virtually directly applicable, it was utilized for this study.

Under normal shipping conditions, the cask is filled with water (or a substitute low freezing point liquid), which maintains the temperature below 192°F. Since this is well below the normal reactor operating temperature of 463°F, there is no danger of failure at this point. Under the emergency conditions considered for the remainder of this section, it was assumed that the coolant was lost for a period of 48 hours. By the conservative application

of the Battelle data for this time period, it was found that a safe design temperature would be 950°F. Thus, by applying a 200°F factor of safety, a recommended upper limit for the fuel elements would be 750°F. The details of this evaluation are presented in the following section.

3. Calculations - In utilizing the failure theory proposed in reference VII-2, several conservative assumptions are made. These assumptions are:

(1) A 30 w/o UO_2 matrix compared to the 28.3 w/o UO_2 matrix of PM-1.

(2) Three years of operation of the fuel element at a constant maximum temperature versus the actual two years of PM-1 operation at full power.

(3) Fuel elements operating at a constant temperature of 625°F over the reactor cycle. This is the maximum temperature that would be felt including water channel peaking and is considerably above the average.

(4) A burn-up factor of 0.8 was assumed. Since the ratio of fission to total (fission plus absorption) cross-section is approximately 0.84, this assumption is quite conservative and virtually impossible to obtain in practice. The average burn-up for the reactor is 0.3

(5) The design limit utilized in the BMI report referenced is that recommended for a safe design and is not immediately adjacent to an expected failure point.

If a fuel specimen is irradiated for extended periods at uniform elevated temperatures, it will undergo creep deformation.

Although the stress distribution in a dispersion type element is complex, it is assumed that the dependence of the overall creep rate on stress and temperature will be of the same form as for uniaxial tension. No attempt is made to determine the spatial stress distibution in the cermet. A term α is found which is a function only of the total creep and the structure of the specimen. the term α is related mathematically to the parameters of burn-up, temperature and time. The values of α obtained from a number of different experiments on identical specimens may be used to compare the relative severity with respect to creep of the different tests. It is then possible to obtain experimental correlations between the test parameters and the value of α at specimen failure.

Referring to the Battelle report, the value of α suggested as a maximum for a safe operating limit is 10^{13} (Ref. VII-2, P.14) Computing a value for α over the lifetime of the core during operation by means of equation 10 on p. 5 of reference VII-2:

$$\alpha = \frac{1}{5.46} (B_f\theta)^{4.46} t_f \exp \left[-3.1 \times 10^4 \left(\frac{1}{\theta} - \frac{1}{1560}\right)\right], \theta \leq 1560°R$$

Where B_f = 0.8 (maximum burnup)

θ = 1085°R (625°F)

t_f = 1095 days (3 years)

$\alpha_{oper.} = 4.5 \times 10^{11} = .045 \times 10^{13}$

Subtracting this from the total maximum allowable, which is 10^{13}:

$$\alpha_{avail.} = 10^{13} - .045 \times 10^{13} = .955 \times 10^{13}$$

This is the value of α available for the post irradiation over-temperature condition.

Referring to equation 9 on p. 5 of reference VII - 2,

$$\alpha = \int_0^{t_f} (B\theta)^{4.46} \exp\left[Q_i \left(\frac{1}{\theta} - \frac{1}{1560} \right) \right] dt$$

Where α allowable $= .955 \times 10^{13}$

$B = 0.8$ (constant)
$\Delta t = 2$ days (48 hours)

Since Q_i, B & θ are constants

$$\alpha = (B\theta)^{4.46} \exp\left[Q_i \left(\frac{1}{\theta} - \frac{1}{1560} \right) \right] \Delta t$$

$$\therefore \quad .955 \times 10^{13} = B^{4.46} \Delta t \; \theta_{max}^{4.46} \exp\left[-3.11 \times 10^4 \left(\frac{1}{\theta} - \frac{1}{1560} \right) \right]$$

Thus, the calculated value of θ max is:

θ max $= 1410°R = 950°F$

Therefore, based on the conservative assumptions used, the maximum fuel temperature allowed to preclude failure is 950°F. To meet the fuel element temperature criterion, therefore, the maximum allowable fuel element temperature is 750°F, which is 200°F below the predicted safe value.

B. Activity Release Rates

Under accident conditions, it is assumed that 5% of the fuel elements break into sections one foot long. The 5% corresponds with the requirements specified by the spent fuel shipping regulations for the dispersion type fuel elements used in the PM-1 type reactors. Under these conditions the criteria to be met are:

(1) Under normal temperatures the I-131 release to air must be less than 10 curies in 10 minutes.

(2) Under maximum temperature conditions (loss of coolant) the release must be less than 100

curies of I-131 in 48 hours. The activity must also include less than 10 curies of beta plus gamma activity due to gaseous products excluding Xe, Kr, and I-131 and also less than 0.1 curie of alpha activity.

Because of both shield weight limitations and limited site access for the PM-1 type plants, it is necessary to cool the core down for a minimum period of one year prior to removal. After the one year cool-down period, the following activity levels exist in the core. These data are based on an extension of the work presented in references VII-3 and VII-4.

(1) Total I-131 activity is reduced to a negligible level due to it's short half-life.

(2) Total beta plus gamma activity due to gaseous products, excluding Xe, Kr, and I-131 is reduced to less than 1 curie.

(3) Total alpha activity is reduced to a negligible level due to radioactive decay.

Therefore, all of the activity limitations under accident conditions are readily satisfied because the total activity existing in the core in the various categories is less than the limits required.

VIII CRASH FRAME DESIGN ANALYSIS *

The purpose of the crash frame is to maintain the cask cover in place in the event of an accident in which the cask is subjected to a 30-foot free fall. It is assumed that at impact the cask has tilted upside down--since the cask cover tends to come off in an impact of this type and stay on if the cask hits on its bottom. The frame is designed to resist a vertical impact and also an impact at 45 degrees.

A schematic drawing of the cask and frame is shown in Fig. VIII-1. In this figure, the cask is tilted upside down as it would appear in a vertical impact.

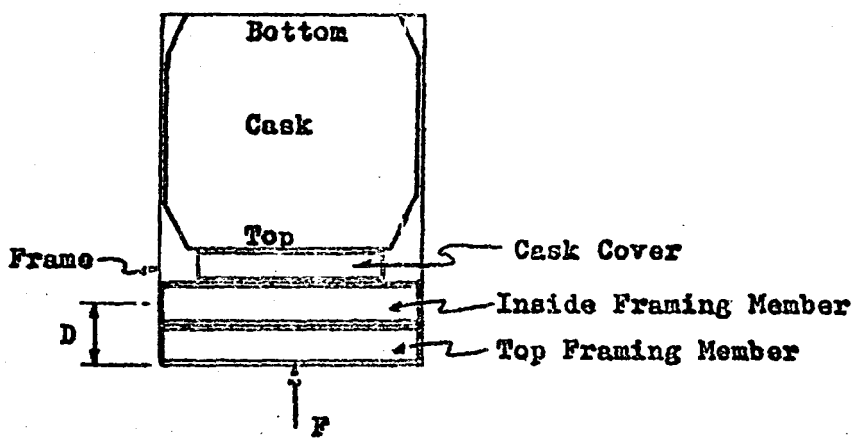

FIG. VIII-1 SCHEMATIC DIAGRAM OF CASK AND FRAME

The estimated weights of the various parts of the cask and frame are shown below:

Total cask weight (including cask, contents, and protection frame): W = 32,500 pounds.

Cask cover weight and contents, W_c = 4,070 pounds.

The basis of the frame design is to provide structural framing members on the top of the cask which upon impact will deform and absorb

* This chapter was prepared for the Edlow Lead Company by Battelle Memorial Institute and submitted to The Martin Company.

the impact energy. There are two approaches that might be taken in the design of these structural members. Very heavy, thick members can be provided which will act elastically and have no permanent deformation. This will mean that the bolts holding the cover would be subjected to high loads because of the small deformation distances. The second approach is that lighter structural members can be provided which will permanently deform during impact and thus provide a large deformation distance which tends to lower the forces on the cask cover bolts. The second approach has been chosen as being less expensive and more practical.

A. Basic Relationships

The total kinetic energy attained by the cask in free fall must be absorbed by the cask frame if it is to protect the cask during impact. Therefore, a relationship can be established between the impact forces and the energy.

The kinetic energy attained by the cask during free fall is WH, where H is the height of fall (30 feet) and W the weight of the cask. Assuming that the resisting force of the frame F is constant throughout the time of impact, the energy absorbed by the frame is FD, where D is the deformation distance. Assuming F is a linearly variable force, the energy absorbed by the frame is FD/2. Both assumptions are approximations but they should yield results of sufficient accuracy.

If the frame absorbs the entire energy of impact, the following conditions must be met:

For a constant force F_1,	$WH = F_1D$	(1)	applies to vertical impact
For a linearly variable force F_2,	$WH = 1/2\ F_2D$	(2)	applies to 45° impact

B. Determination of Frame Deformation

Now that the equations have been established relating the kinetic energy of the cask to the resisting force of the cask frame and its deformation, it is possible to calculate the frame deformation once the resisting force of the frame is known.

1. Buckling Stress Relationships - The method of determining the resisting force of the frame is based on the buckling strength of the members. Because of the geometrical arrangement of the members, the portions which will buckle are the webs. The problem, therefore, is reduced to determining the buckling strength of a plate.

The elastic buckling stress can be calculated from the general formula shown below (Ref: VIII-1, VIII-3, VIII-4):

$$\sigma_{cr} = KE\left(\frac{t}{b}\right)^2$$

Where K is a constant depending on the boundary conditions and the plate dimensions a and b. (K = 7.0 for the members under discussion.)

b is the loaded length of the plate

t is the plate thickness

E is the modulus of elasticity

The structural members which deform are the top and inner framing members, shown in Fig. VIII-1. These members are 12 I 35 beams, made of ASTM A7 structural steel. Their dimensions and support conditions are shown in Fig. VIII-2.

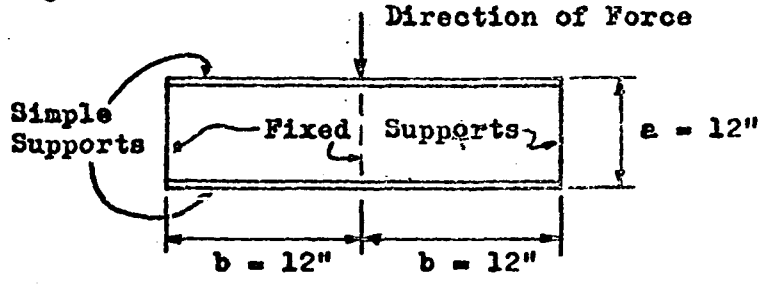

FIG. VIII-2 GEOMETRY OF FRAMING MEMBERS

The value of the elastic buckling stress is:

$$12 \text{ I } 35, \quad \sigma_{cr} = KE\left(\frac{t}{b}\right)^2 = 7.0\ (30 \times 10^6)\ \left(\frac{.423}{12}\right)^2 = 268{,}000 \text{ psi}$$

This value is above the yield strength (*) of the A-7 steel which has a yield strength of 54,000 psi under the impact conditions, as shown in the Appendix to this chapter. Therefore, this equation does not apply in this inelastic region and the stress σ_{cr} calculated above is not applicable. It does indicate that permanent (plastic) deformation will take place and that the buckling strength must be determined on the basis of the plastic buckling behavior of the material.

The buckling equation (Ref. VIII-1) which is applicable in the plastic range is:

$$\sigma'_{cr} = KE\sqrt{\tau}\left(\frac{t}{b}\right)^2 \qquad (3)$$

Where $\tau = E_t/E$

E_t = tangent modulus at the corresponding stress σ'_{cr}.

The buckling stress σ'_{cr}, is related to the yield stress by the factor τ. Since the frame is designed to provide a large (plastic) deformation, the highest yield strength of the material should be used in calculating the buckling strength of the members. However, since the yield strength is dependent on the strain rate, the specific yield strength which should be used is unknown because the characteristics of the material on which the cask may fall are not known. Maximum and minimum limits of the yield strength, however, have been defined in the Appendix. These are 33,000 psi and 54,000 psi. In order to insure that the frame can provide adequate deformation in all circumstances, the lowest yield strength will be used and a comparison made for the higher yield strength.

---

* In a standard tensile test the yield strength is 33,000 psi.

2. Deformation in Vertical Impact - The resisting force F which can be supplied by the frame is calculated by computing the buckling stress of the members and, then, total force available from the frame.

Rearranging the terms of Equation (3) as shown below, if the left-hand side of the equation is computed then σ'_{cr} can be found in Table 27 on page 343 of Reference VIII-1.

Thus, for the structural member of interest:

$$\frac{\sigma_{cr}'}{\sqrt{\tau}} = KE\left(\frac{t}{b}\right)^2$$

12 I 35, $\frac{\sigma_{cr}'}{\sqrt{\tau}} = KE\left(\frac{t}{b}\right)^2 + 7.0\ (30 \times 10^3)\ \left(\frac{.428}{12}\right)^2 = 268$ ---- $\sigma_{cr}' = 32{,}900$ psi

The stress value can be converted to a value of load per inch of plate length by multiplying it by the plate thickness, as shown below:

12 I 35, $q = 32{,}900\ (.428) = 14{,}100$ lb/in.

The computed q is the plastic buckling load per inch of plate length for a yield strength of 33,000 psi.

Now that this value has been determined, the deformation of the frame for a vertical impact can be computed from Equation (1) as follows:

$$D = \frac{WH}{F_1} = \frac{32{,}500(360)}{1{,}355{,}000} = 8.65 \text{ inches}$$

Where H = 30 feet or 360 inches

F_1 = (no. of beams) (total length) (q of 12 I 35)

= 4(24) (14,100) = 1,355,000 lb/in

For the higher yield stress, the deformation D' is approximately

$$D' = \frac{\text{lower yield}}{\text{higher yield}} (D) = \frac{33}{54} (8.65) = 5.28 \text{ inches}$$

Therefore, the deformation of the crash frame in a vertical impact will be between 8.65 and 5.28 inches. In either case the deformation will be confined to the 12 I 35 top framing member.

3. Deformation in 45-Degree Impact - Similar calculations can be made to determine the deformation in a 45-degree impact except that Equation (2) is used because of the variable nature of the force.

$$1/2\ F_2 D = WH$$

$$889{,}000\ D = 4{,}075{,}000 = 32{,}500\ (360)$$

$$D = 17.7 \text{ inches}$$

Where: $1/2\ F_2 D$ for the various members is:

Inside member $1/2\left[58(14{,}100)\right] (D-8.5)$

Top member $1/2\left[58(14{,}100)\right] (8.5) + \left[54(14{,}100)\right] (D-8.5)$

Total $1/2\ F_2 D = 889{,}000\ D - 4{,}075{,}000$

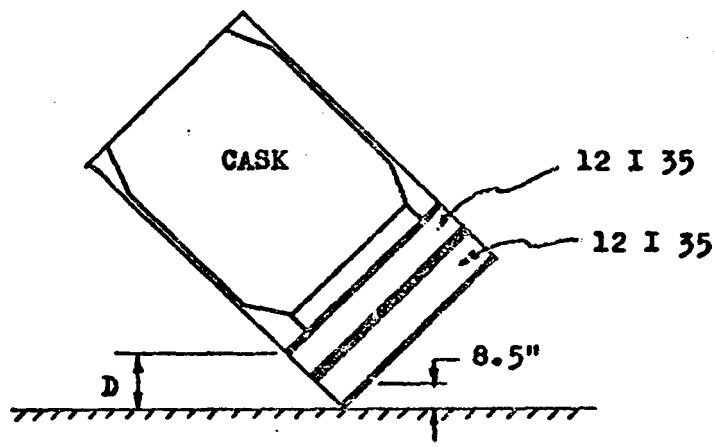

FIG. VIII-3 SCHEMATIC OF CASK IN CORNER IMPACT

For the higher yield strength, the deformation D' is approximately

$$D' = \frac{\text{lower yield}}{\text{higher yield}} (D) = \frac{33}{54} (17.7) = 10.8 \text{ inches}$$

which in either case is satisfactory since approximately 17.7 inches have been provided for deformation.

C. Stresses in Cover Bolts

The geometrical arrangement of the framing members, shown on Martin drawing 372-2106016 is such that the framing members on the top of the cask bear directly on the cask cover. During an impact, the forces are transmitted directly to the cask cover and maintain it in place. Therefore, the stresses in the cover bolts are very low in an impact, but are not directly calculable.

If it is assumed, however, that the framing members have become separated from the cask cover (which is unlikely), then the stresses in the bolt can be checked. The only purpose in making this computation is to show that the stresses in the bolts are below the ultimate strength of the material and that they will not fail.

The stresses in the cover bolts can be computed once the forces on the bolts are known. The forces on the bolts can be determined from Newton's second law, $F_b = \frac{Wc}{g} a_c$, where g is the acceleration of gravity, W_c is the weight of the cask cover and the contents, and a_c is the acceleration of the cask cover.

It can be assumed that the acceleration of the cover is the same as that of the cask for the case when the bolts remain intact. The force on the bolts can then be determined as follows:

$F = \frac{W}{g} a$ a = acceleration of cask

$$\text{Since } a = a_c = \frac{Fg}{W} = \frac{F_b g}{Wc}$$

$$F_b = F \frac{Wc}{W}$$

Since the maximum force F occurs during the smallest deformation, this value of F will be used.

$$F = \frac{WH}{D} = \frac{32,500(360)}{5.28} = 2,220,000 \text{ lb.}$$

The force on the cover bolts F_b is, therefore,

$$F_b = F \frac{Wc}{W} = 2,220,000 \left(\frac{4070}{32,500}\right) = 278,000 \text{ lb.}$$

Where $W_c = 4070$ lb

Since there are 12 bolts, the force per bolt is 278,000/12 or 23,200 lb per bolt. The stress on each 1-inch-diameter bolt is 23,200/0.551 or 42,000 psi-- such stress is below the ultimate strength of Type 304 stainless steel.

D. Frame to Cask Attachment

1. Member Size - The crash frame legs hold the crash frame to the cask during impact and lifting of the cask. Since the largest force occurs during impact, the selection of frame leg sizes has been based on that portion of the impact load which is not supported directly in bearing on the cask top.

At each leg there is approximately 10 inches of the inner framing member which is not bearing directly on the cask top (see Martin drawing 372-2106016).

Therefore, the load P, which each leg supports is the buckling load of the framing member per unit length multiplied by the unsupported length.

$$P = (14,100)(10) = 141,000 \text{ lb.}$$

The required cross-sectional area of the leg is the load P, divided by the stress, which is taken here as the lower yield stress (33,000 psi) to be on the safe side.

$$\text{Area of leg, } A = \frac{141,000}{33,000} = 4.27 \text{ sq. in.}$$

A convenient member size is a 6 WF 25 which has a cross-sectional area of 7.35 sq in.

2. Attachment Bolts - The number of bolts used to fasten the frame leg to the cask is based on the maximum load that can be carried by the leg.

The maximum load is the higher yield stress multiplied by the area of the leg member. Therefore,

$$P_{max.} = 54,000 \ (7.35) = 397,000 \text{ lb.}$$

Four 1-inch-diameter ASTM A-325 bolts are required to withstand P_{max} as shown below:

Load per bolt = 2 (area) (ultimate strength) = 2 (0.785) (80,000)* = 125,600 lb.

No. of bolts = 397,000/125,600 = 3.2, use 4.

E. Appendix

Yield Strength of Material At Impact

The material under consideration is ASTM A-7 structural steel. The yield strength of A-7 steel as measured in an ordinary tensile test is 33,000 psi.

---

* See Reference VIII-5

The loading rate or strain rate that is involved in the impact, however, would be considerably greater than that used in a tensile test. Since it is known that increasing the strain rate will also increase the yield strength, this increase should be taken into account in determining whether the buckling stress is above or below the yield stress.

Before it is possible to obtain an estimate of the increased yield strength, it is necessary to obtain an estimate of the strain rate in the impact.

The velocity of the cask at impact for a 30-foot free fall is $v = \sqrt{2gh} = 528$ in/sec. If it is assumed that the cask does not deform the material which it hits, the rate of load application can be determined by multiplying the impact velocity by the effective spring rate of structural members, as follows:

Spring rate, $k = \frac{AE}{L}$

A = cross-sectional area of the structural members

L = vertical height of structural members

Loading rate = $vk = v\frac{AE}{L}$ lb/sec.

To convert the loading rate to the stress rate it must be divided by the cross-section area, A. Finally, to convert stress rate to strain rate it must be divided by the modulus, E.

$$\text{Strain rate} = \frac{vAE}{L}\ \frac{1}{AE} = \frac{v}{L}$$

Which for the structural member involved is

$$\frac{v}{L} = \frac{528 \text{ in/sec}}{20 \text{ in.}} = 26.4 \text{ in/in/sec.}$$

Having the strain rate, it is now possible to determine the

yield strength using the results of an investigation performed by Manjoine (Ref. VIII-2), which shows that for a strain rate of 26.4 in/in/sec the yield strength will be approximately 54,000 psi.

REFERENCES

III - 1 Blomeke, J. O., and Todd, M. F., "Uranium-235 Fission Product Production", ORNL-2127, Part 1, Vol. 2.

III - 2 Rockwell, T., "Reactor Shielding Design Manual", TID-7004, March 1956.

IV - 1 Three Group Neutron Diffusion Calculation (Program F3), XDC 58-7-18, May 1958.

IV - 2 P. Gilmore, Fuel Element Development Study, Part II, Table 3A, Personal Communication, Jan. 16, 1961

IV - 3 APWRC-SYNFAR, A Fortran - II Program for Two - Dimensional Static or Dynamic Synthesis Using P1 or S2 to S16 DSN Flux or Adjoint in Slab, Cylindrical or Spherical Geometry, MND-C-2460, January 1961.

V - 1 Jakob, M., Heat Transfer, Wiley and Sons, Inc., Vol. I, September 1956

VI - 1 McAdams, W., Heat Transmission, McGraw-Hill, 1954, p. 239.

VI - 2 Madison, R. D., Fan Engineering, Buffalo Forge Company, 1949

VI - 3 Etherington, H., Nuclear Engineering Handbook, McGraw-Hill, 1958, pp. 1 - 56

VI - 4 McCabe, W., Smith, J., Unit Operations of Chemical Engineering, McGraw-Hill Book Co., 1956, p. 76, p. 78

VII - 1 ORNL-2902 - "A Failure Analysis For the Low-Temperature Performance of Dispersion Fuel Elements", J. R. Wein, June 15, 1960

VII - 2 BMI-1408 - "A Method of Correlating Irradiation Effects in Dispersion Fuels", Donald Keller, Lewis Hulbert, Bruce Dunnington, January 20, 1960.

VII - 3 Nuclear Science & Engineering, "Energy Release From the Decay of Fission Products", J. F. Perkins and R. W. King, Vol. 3, Number 6, p. 726, June 1958

VII - 4 MND-1721 - "A Program for the Computation of Fission Product Activity", W. D. Owings, March 2, 1959

VIII- 1 Bleich, F., "Buckling Strength of Metal Structures", McGraw-Hill Company, Inc., pp 343-4 (1952).

REFERENCES (continued)

VIII - 2 Manjoine, M. J., "Interference of Rate of Strain and Temperature on Yield Stresses of Mild Steel", Journal of Applied Mechanics, Vol. 11, No. 4, pp A-211 - 218 (December, 1944).

VIII - 3 Roark, R. J., "Formulas for Stress and Strain", McGraw-Hill Company, Inc., pp 312 (1954)

VIII - 4 Peery, D. J., "Aircraft Structures", McGraw-Hill Company, Inc., pp 368 (1950).

VIII - 5 Foreman, R. T. and Rumpf, J. L., "Static Tension Tests of Compact Bolted Joints", ASCE Proc. Vol 86 (ST6), PP 73-100 (June, 1960).